R^3B - SOFIA
Fission Studies

- Collaboration and Experiment
- Physics Goals and Motivation
- S455 Experiment
- Discussion
- Outlook

P. Morfouace *et al.* Nature (April 2025)
DOI 10.1038/s41586-025-08882-7

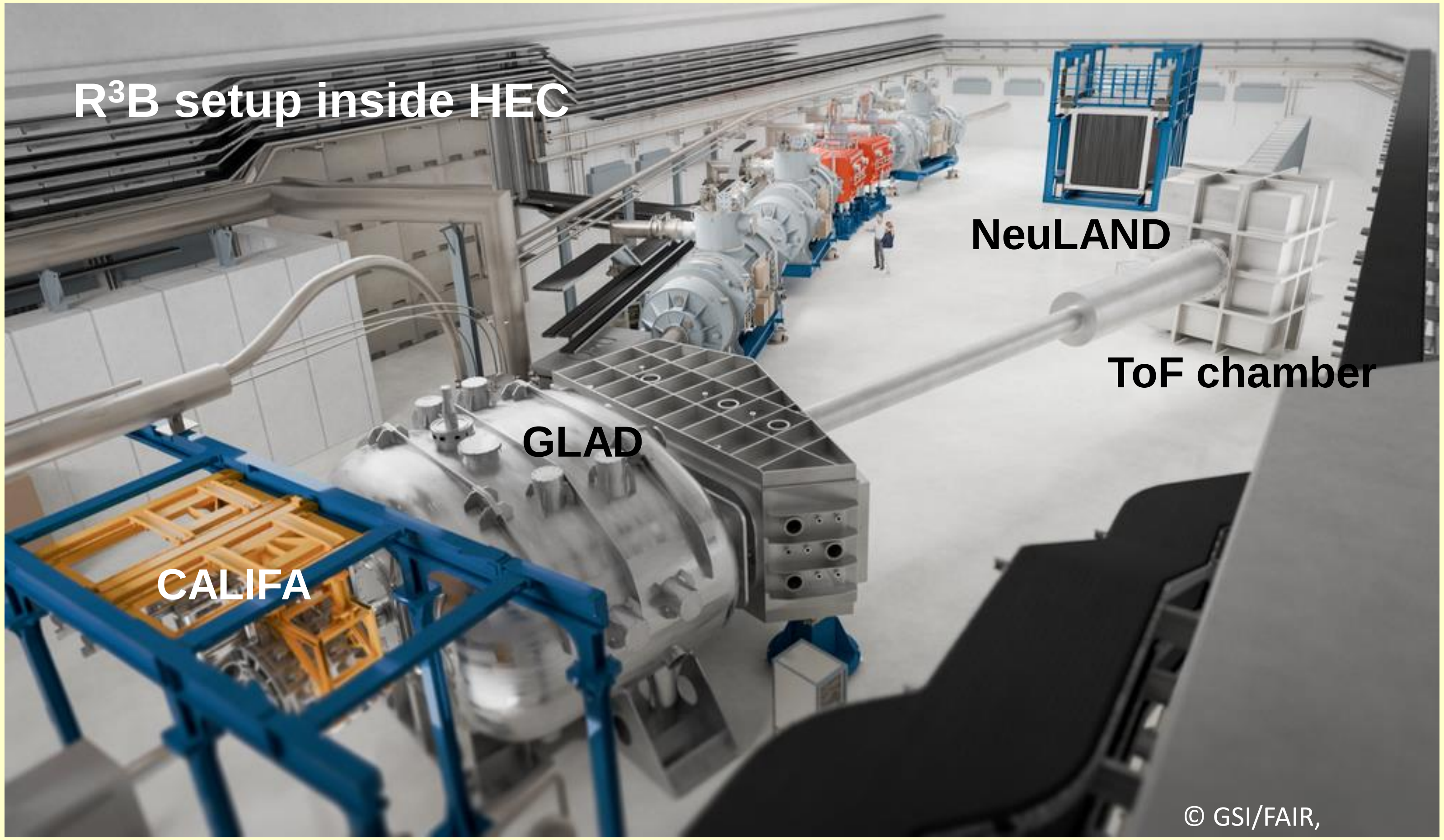

Roman Gernhäuser
Physik Department, Technische Universität München

The Reactions with Relativistic Radioactive Beams Collaboration

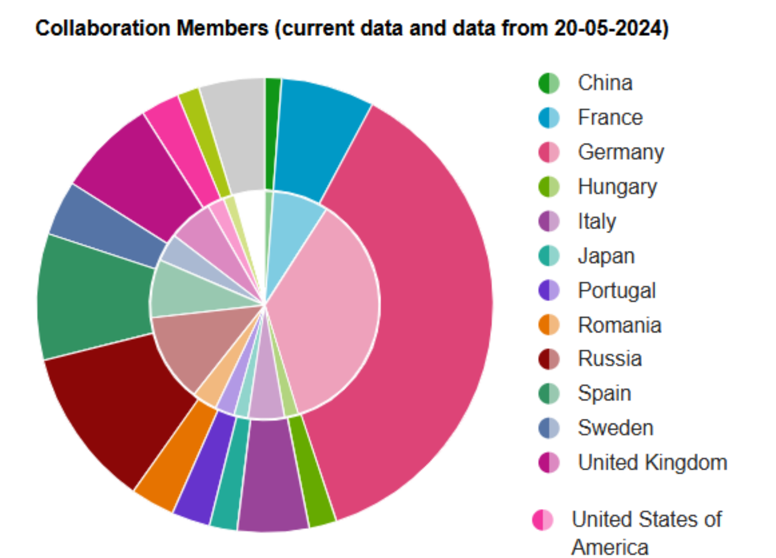

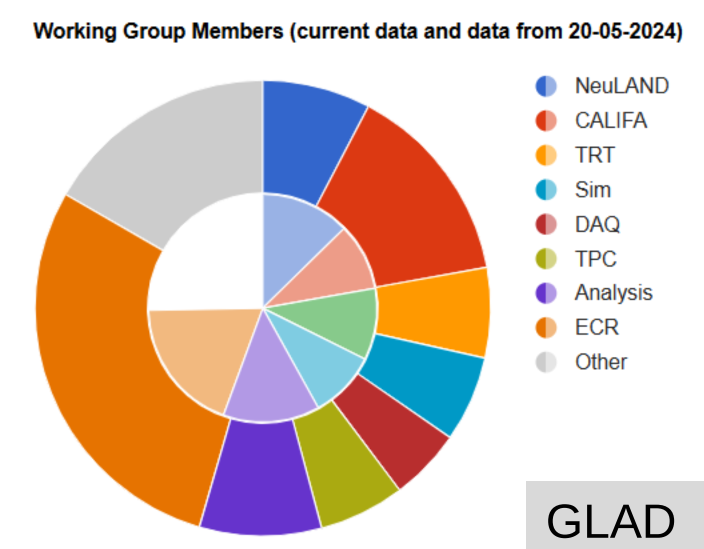

256 active members from
23 different countries and
66 different institutes

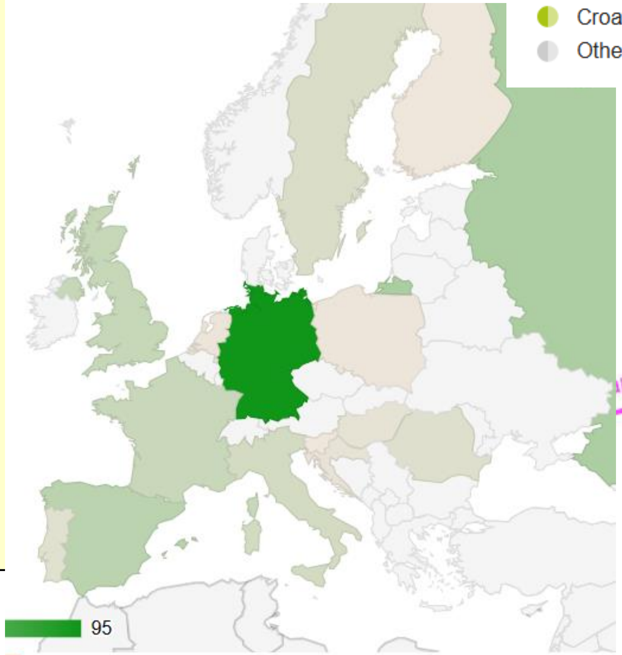

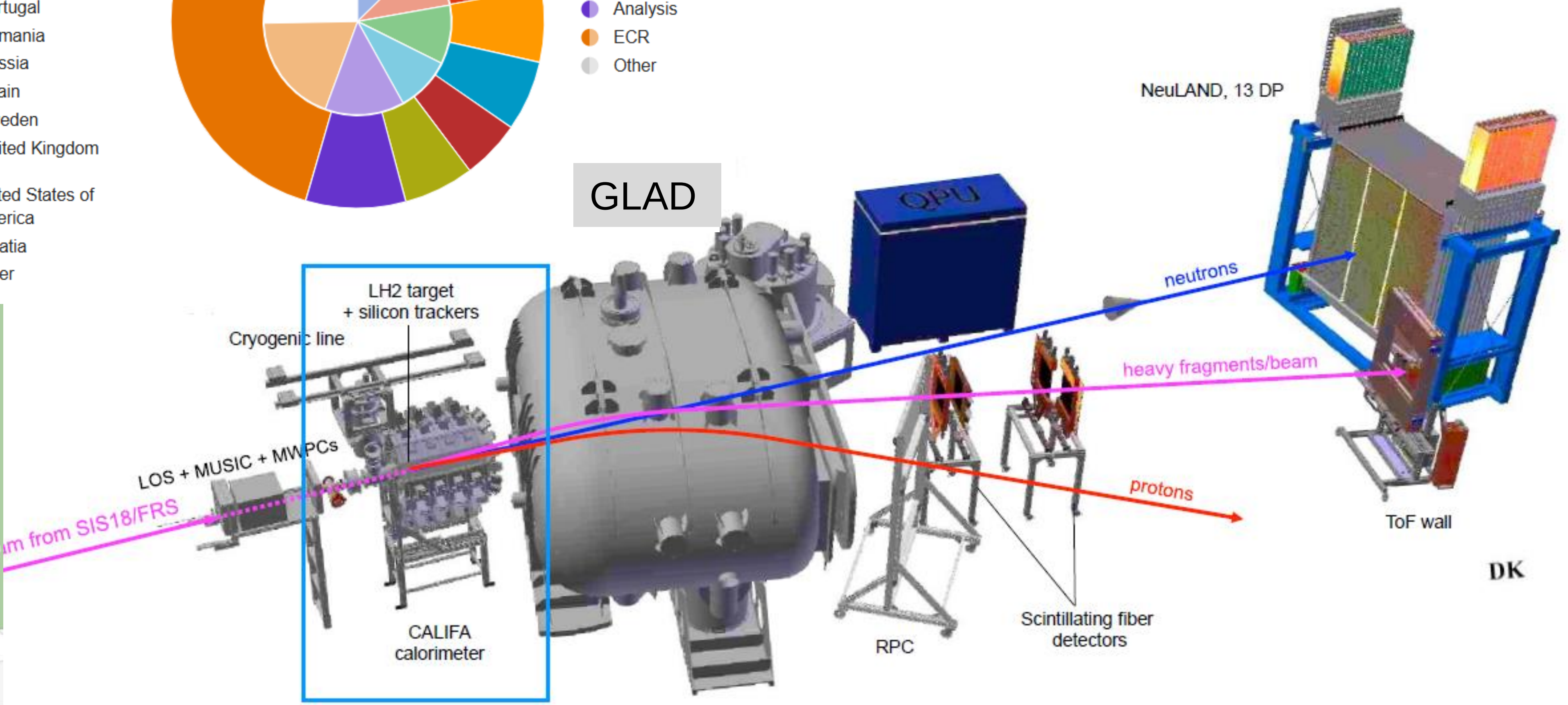

The GSI-FAIR Facility

2019 - 2026

2027 - 2035

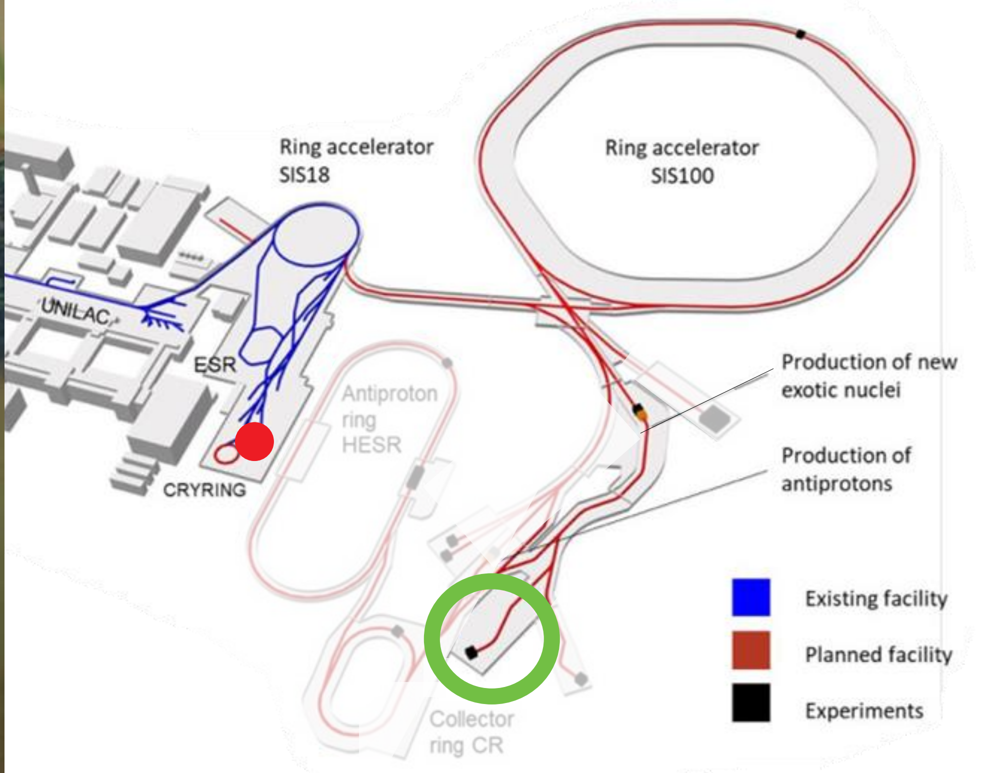

Haik Simon – FAIR & Super-FRS – EPS 20190930

The Fair Facility

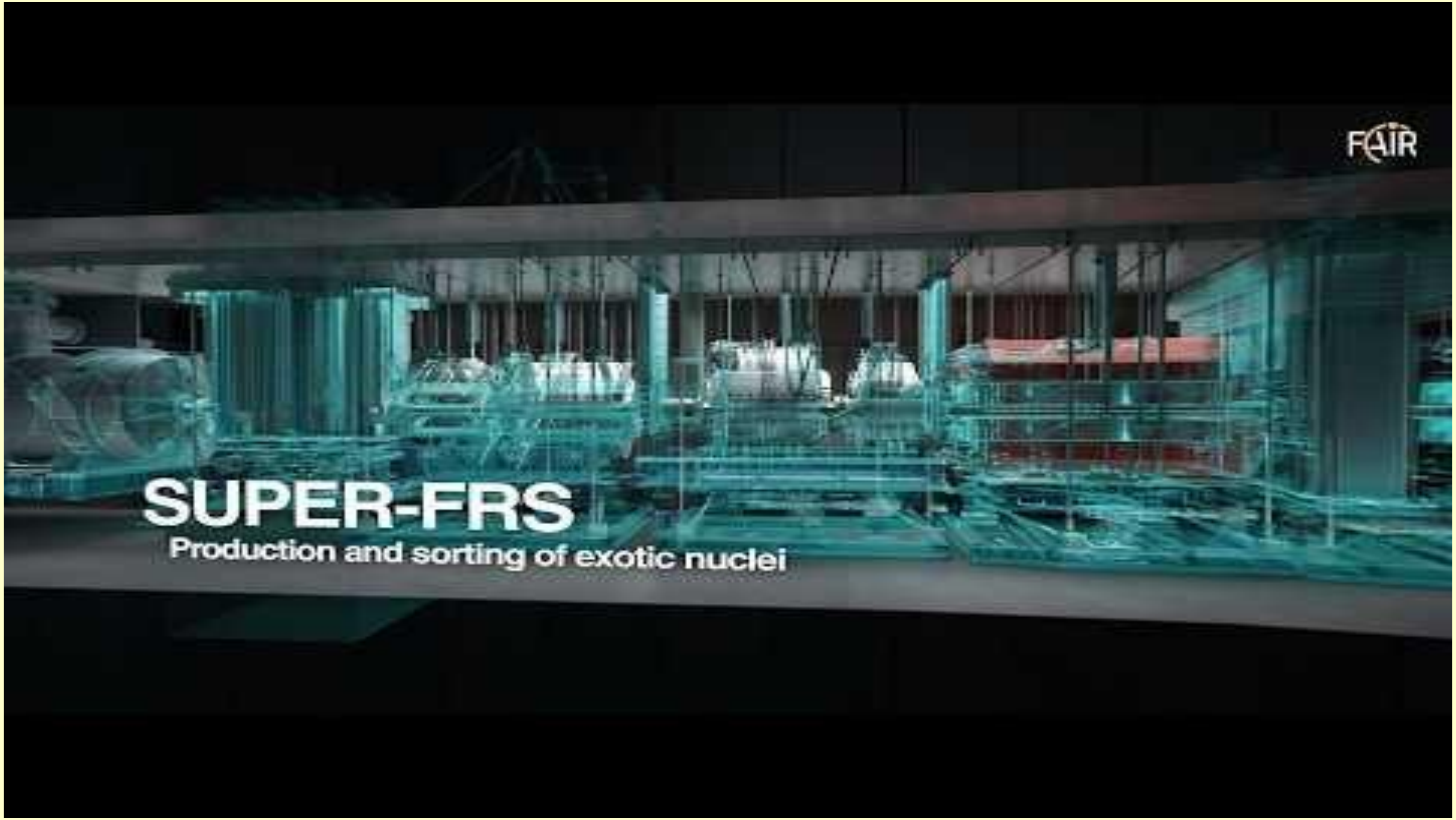

If no Internet

The Cycle of Matter

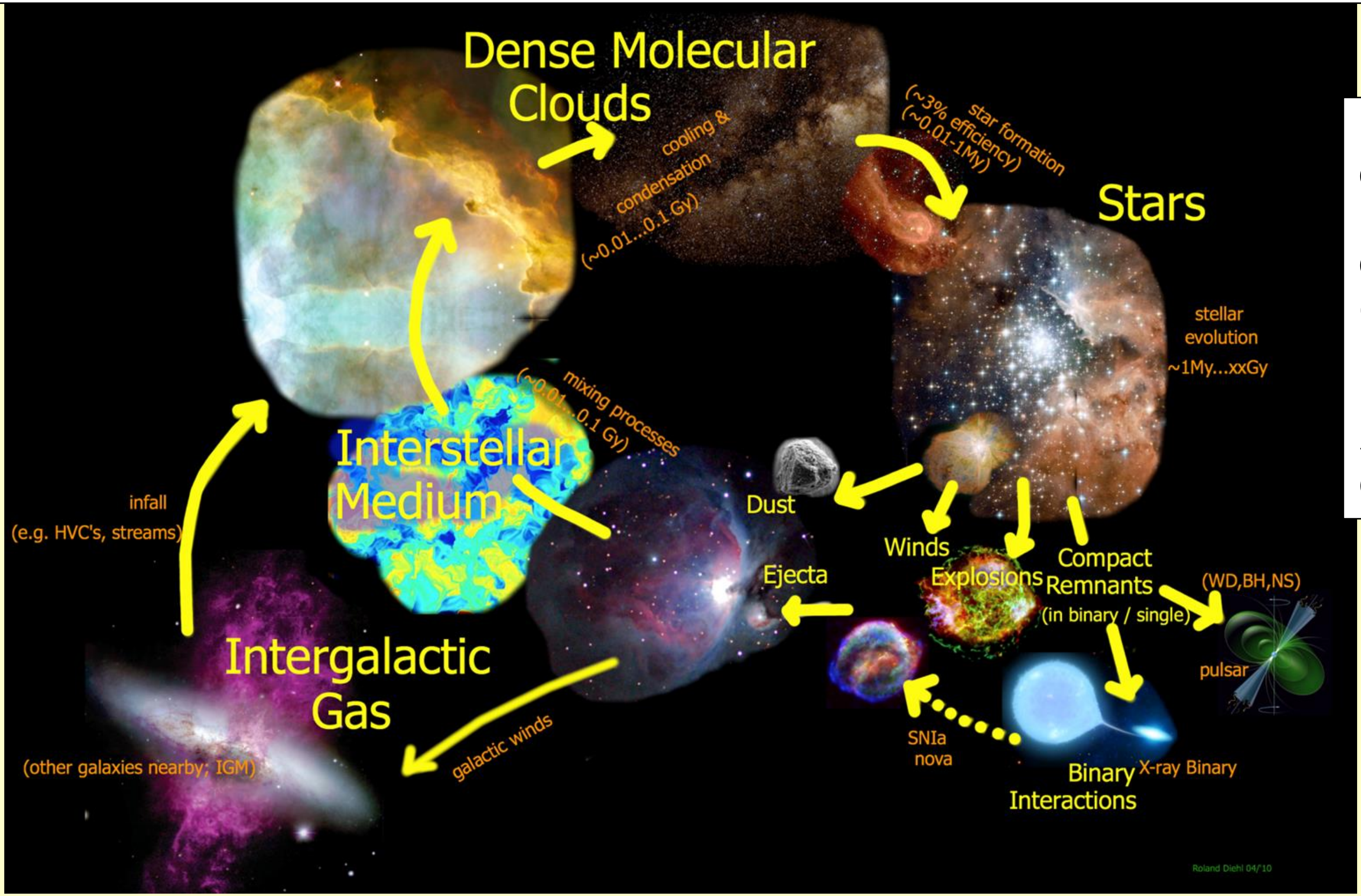

Everything not confined in BHs is recycled continuously (even neutron star matter)

Solar system in Cycle # > 10

Courtesy R. Diehl

Termination of the r-Process

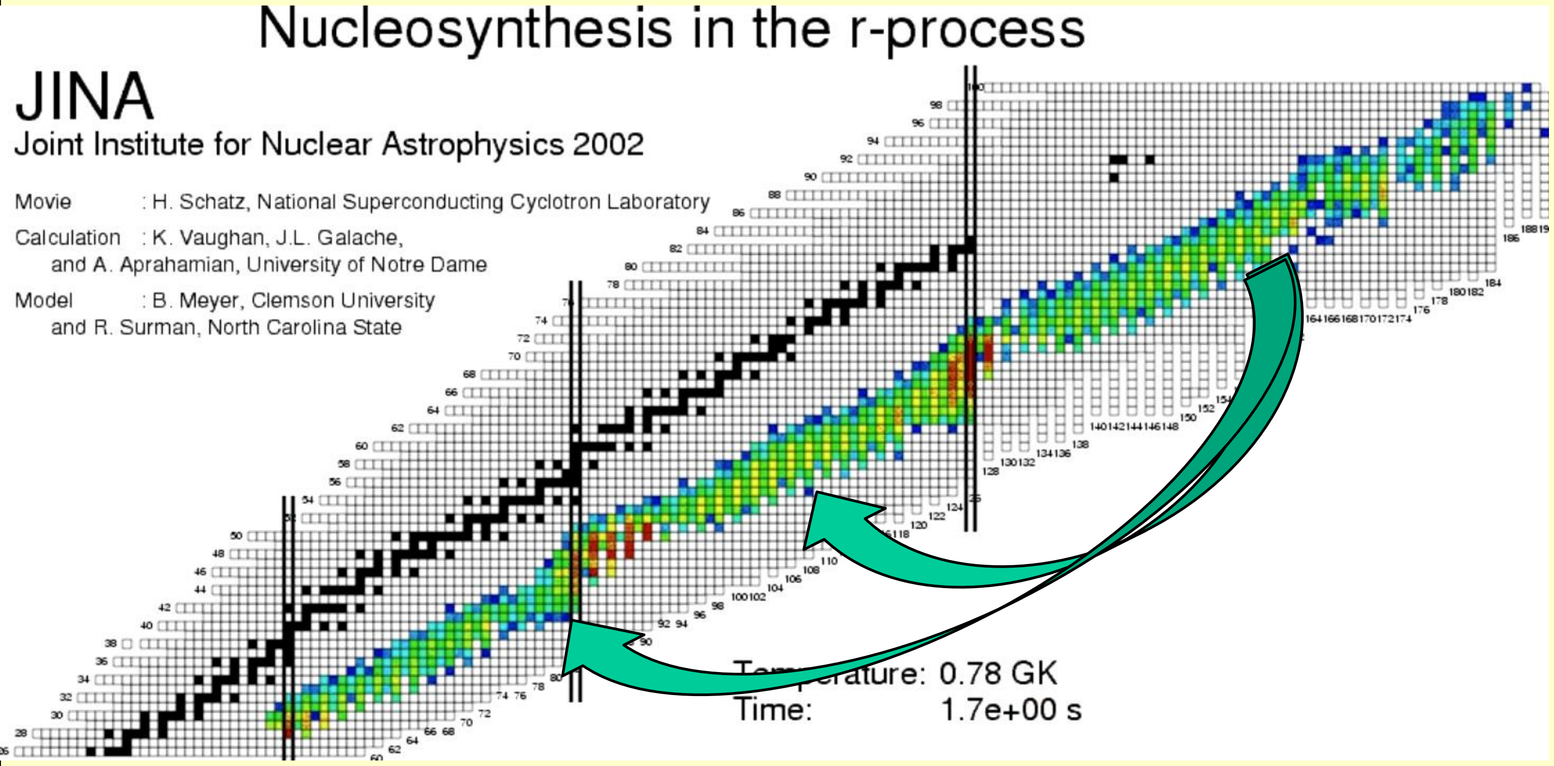

Astrophysical questions: Where is
- the termination of the r- Process ?
- its path on the nuclear chart ?
- new magic numbers?

Experimental cart of nuclides with known fission barriers from (d,p)

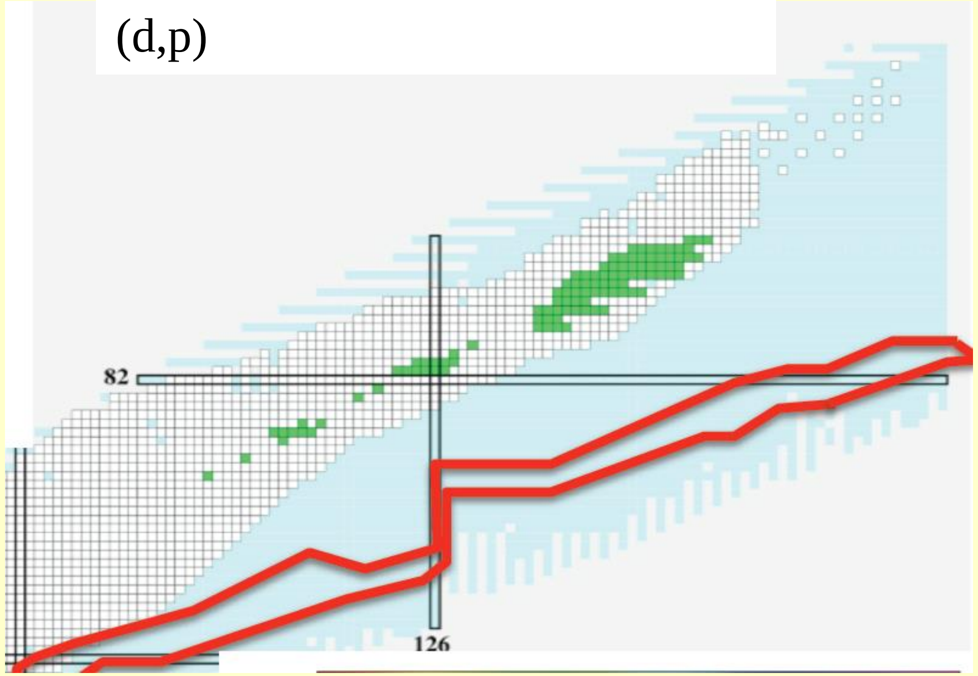

Up to now only studied with classical (d,p) reactions and model calculations.

P. Morfouace *et al.* Nature (April 2025)
DOI 10.1038/s41586-025-08882-7

Experiments until 2023

First indication from
mass Distributions ^{180}Hg
β-decay delayed fission

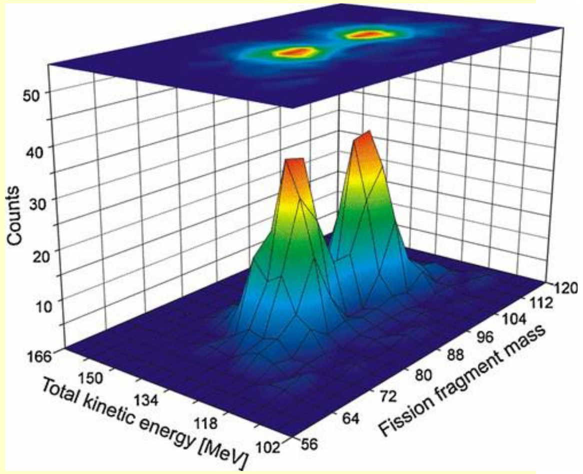

A. N. Andreyev *et al*. Phys. Rev. Lett. **105**, 252502 (2010)

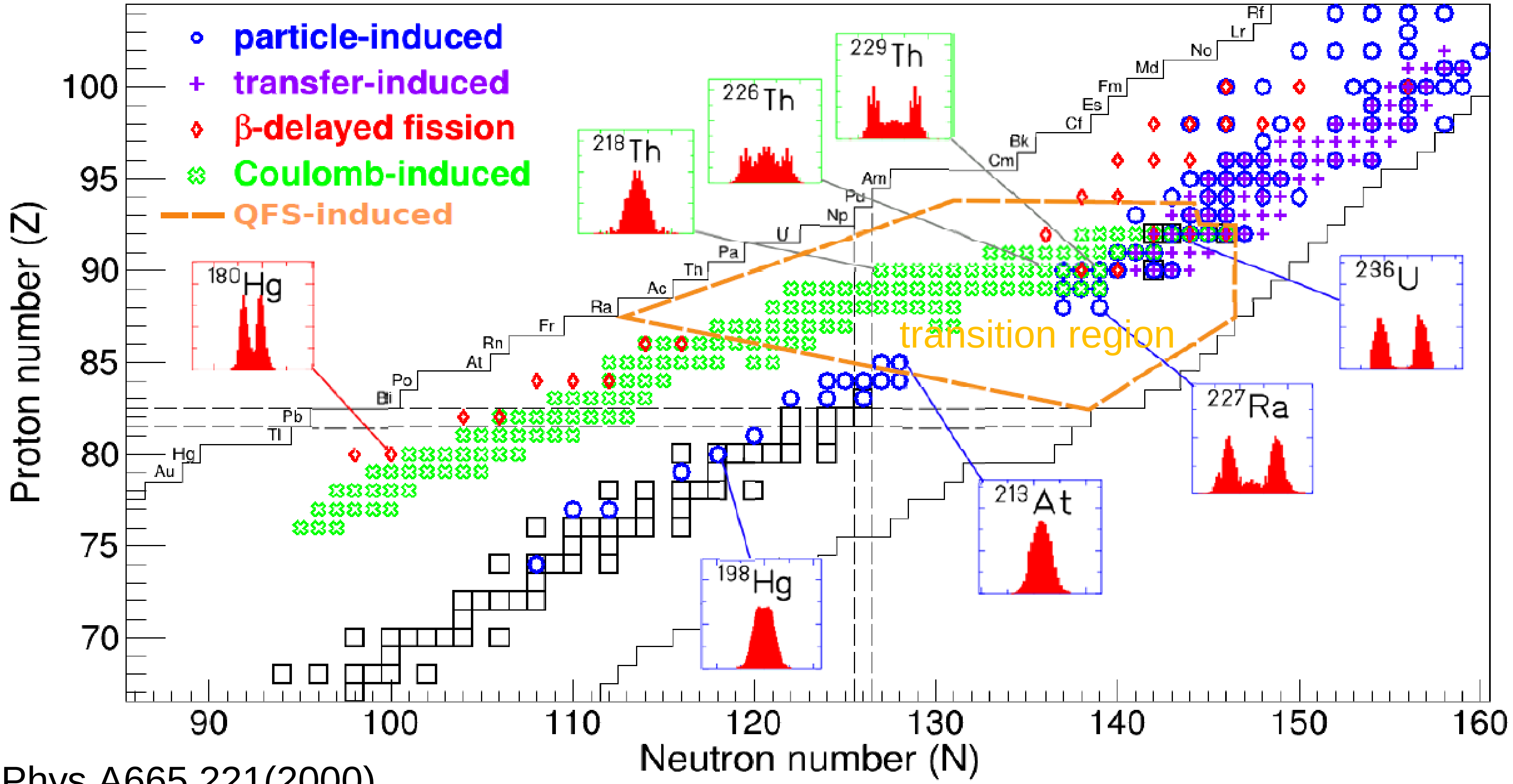

A. N. Andreyev *et al*. Rep. Prog. Phys. **81**, 016301 (2018)

[16] K.H.Schmidtetal.,Nucl.Phys.A665,221(2000)
[17]A.Chatillonetal.,Phys.Rev.C99,054628(2019)
[18]J.F.Martinetal.,Phys.Rev.C104,044602(2021)
[19]A.Chatillonetal.,Phys.Rev.C106,024618(2022)

Impact of Fission on the Element Composition

Science, VOL. 382, NO. 6675, Dec. 2023

NUCLEOSYNTHESIS

Element abundance patterns in stars indicate fission of nuclei heavier than uranium

Ian U. Roederer[1]*†, Nicole Vassh[2], Erika M. Holmbeck[3], Matthew R. Mumpower[4,5], Rebecca Surman[6], John J. Cowan[7], Timothy C. Beers[6], Rana Ezzeddine[8], Anna Frebel[9,10], Terese T. Hansen[11], Vinicius M. Placco[12], Charli M. Sakari[13]

The heaviest chemical elements are naturally produced by the rapid neutron-capture process (*r*-process) during neutron star mergers or supernovae. The *r*-process production of elements heavier than uranium (transuranic nuclei) is poorly understood and inaccessible to experiments so must be extrapolated by using nucleosynthesis models. We examined element abundances in a sample of stars that are enhanced in *r*-process elements. The abundances of elements ruthenium, rhodium, palladium, and silver (atomic numbers Z = 44 to 47; mass numbers A = 99 to 110) correlate with those of heavier elements ($63 \le Z \le 78$, $A > 150$). There is no correlation for neighboring elements ($34 \le Z \le 42$ and $48 \le Z \le 62$). We interpret this as evidence that fission fragments of transuranic nuclei contribute to the abundances. Our results indicate that neutron-rich nuclei with mass numbers >260 are produced in *r*-process events.

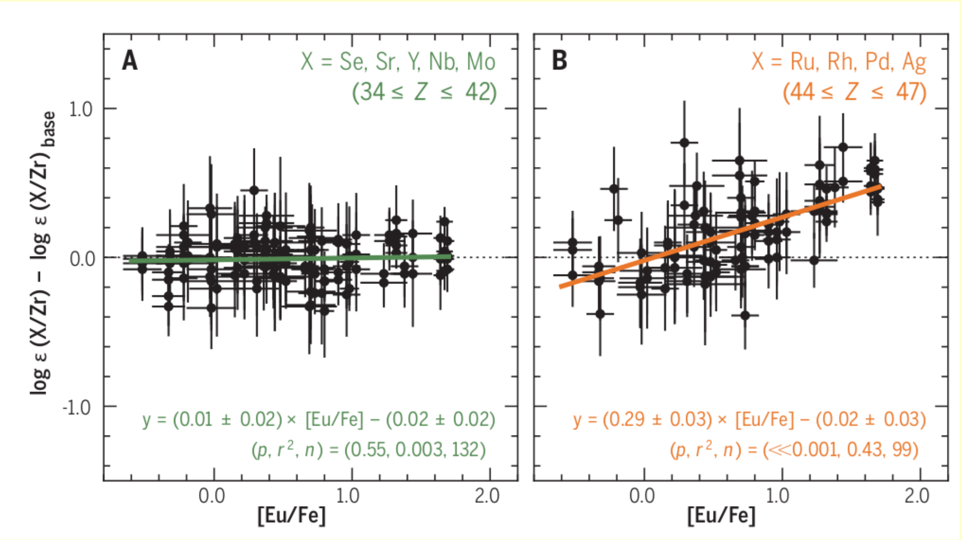

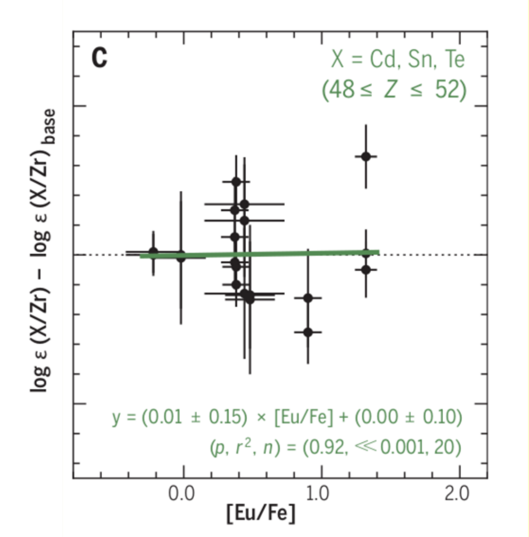

Correlation as a result of asymmetric fission in the Actinides.

Some of them do Spontaneous Fission

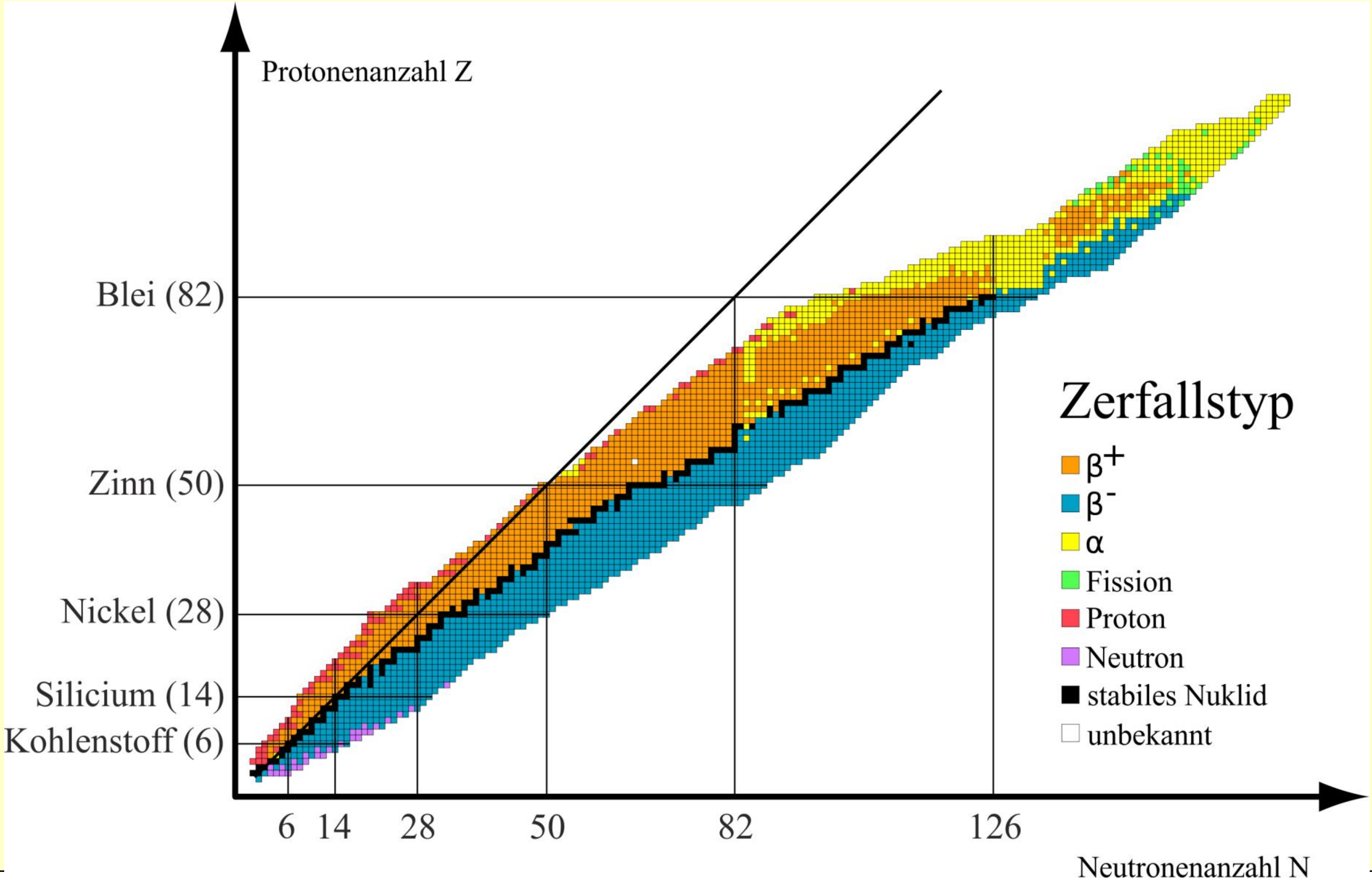

Why is Fission not so Simple?

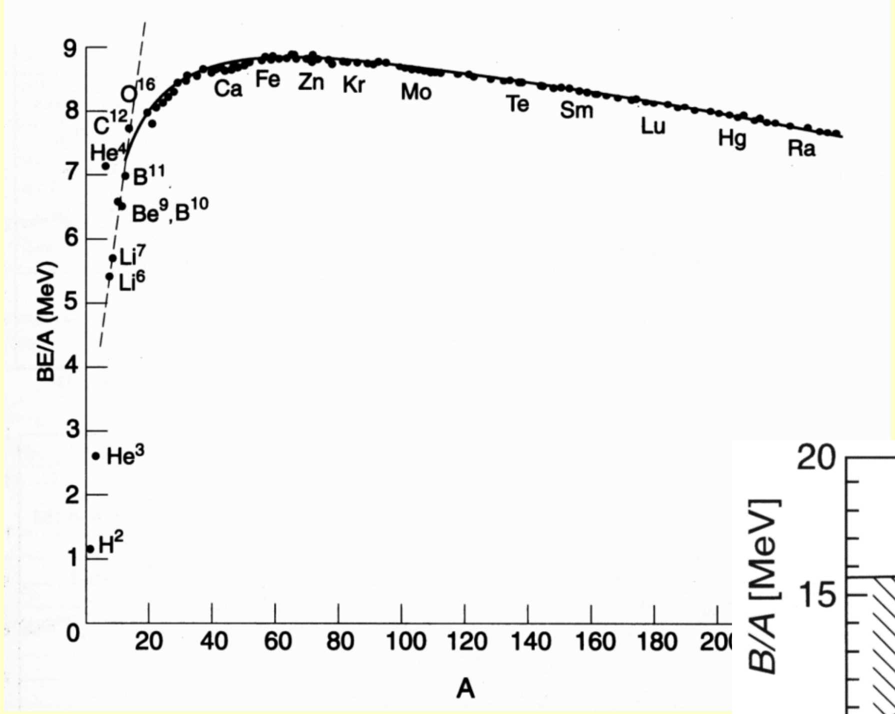

Weizäcker’s liquid drop model

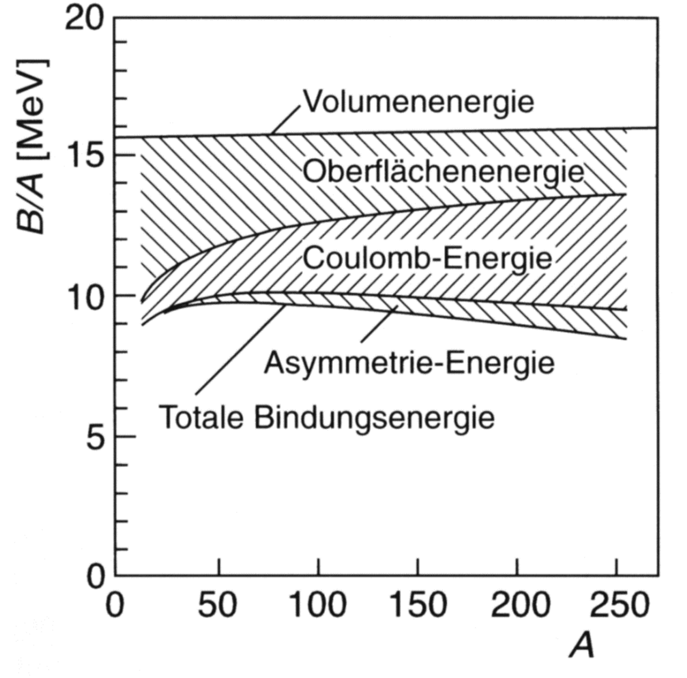

The system is a several step process

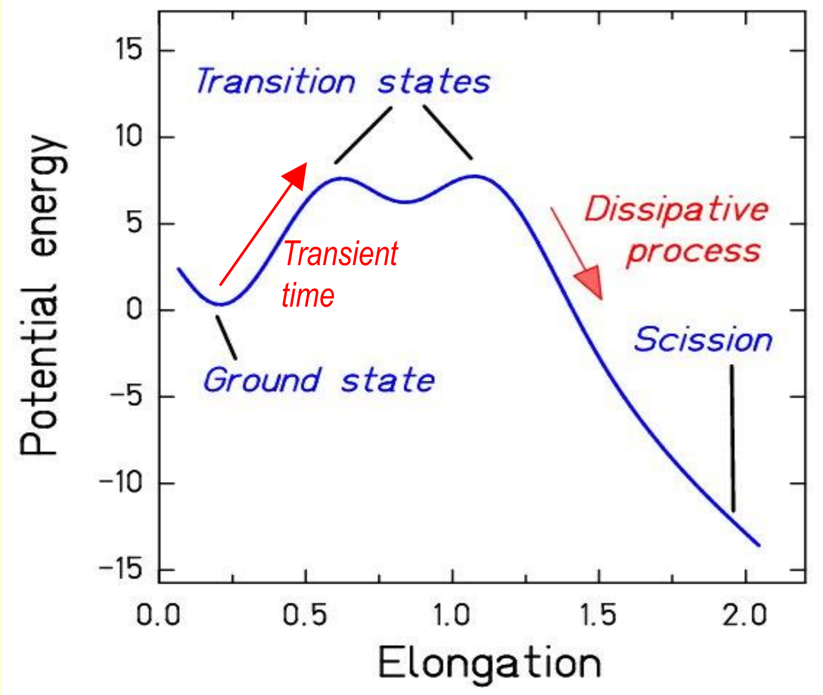

Coupling between intrinsic and collective degrees of freedom

Low Energy Excitation

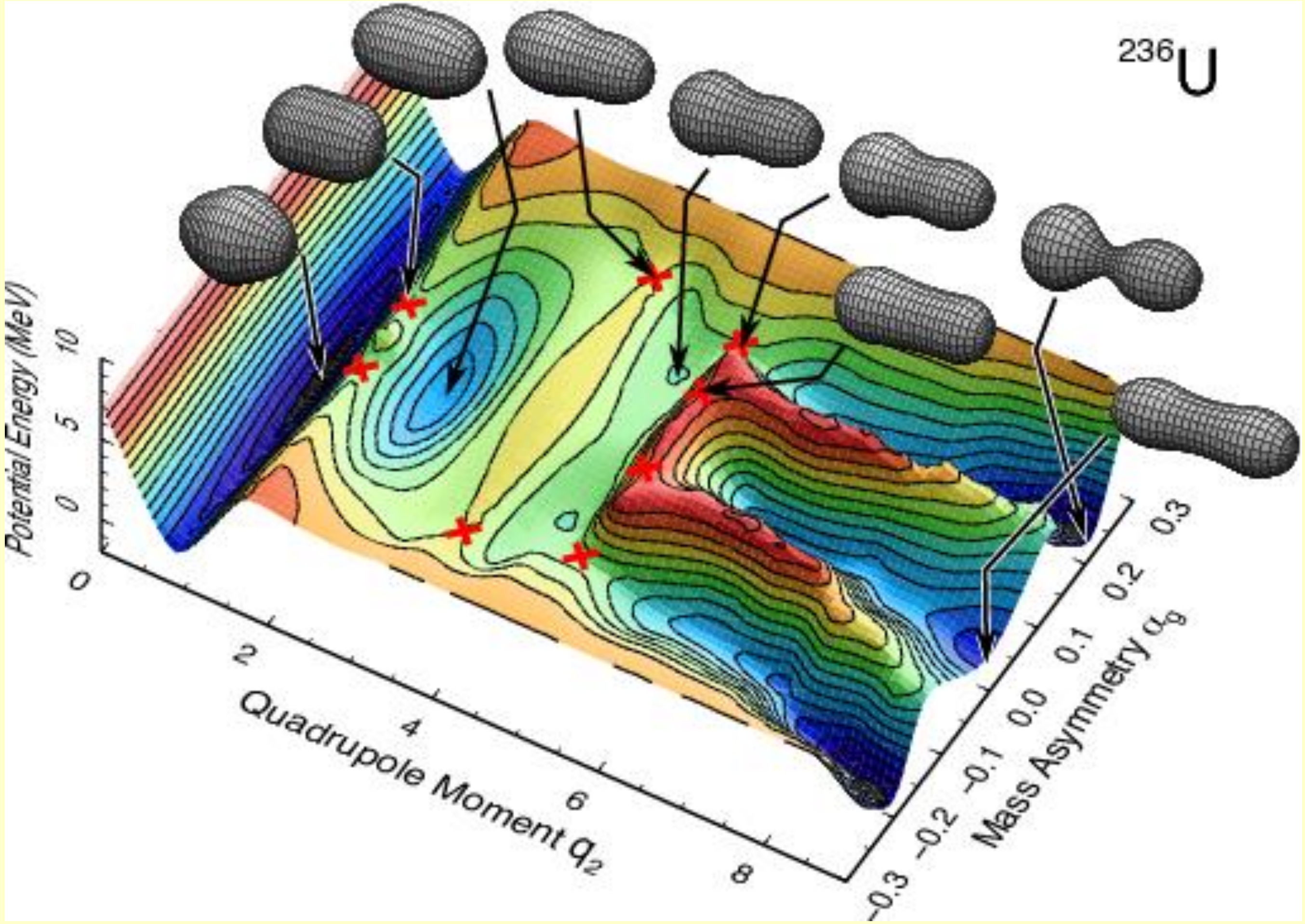

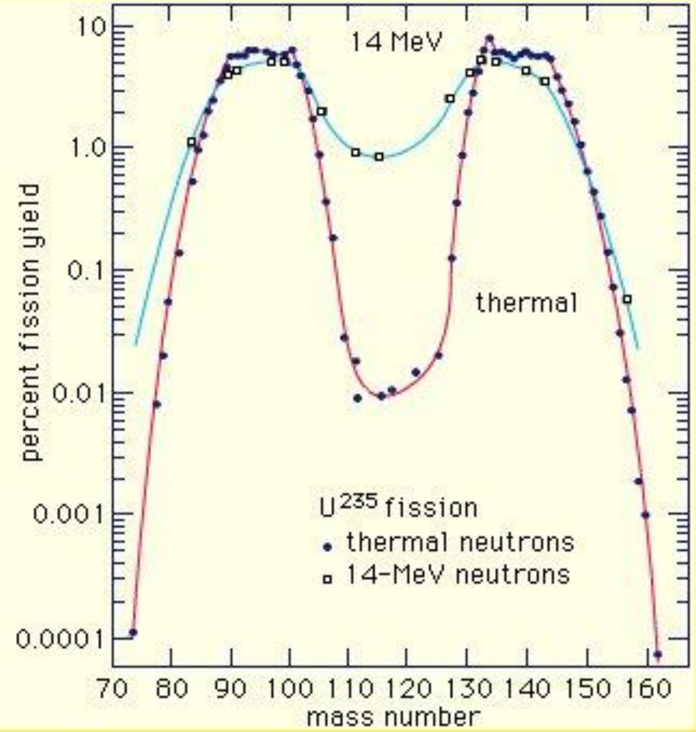

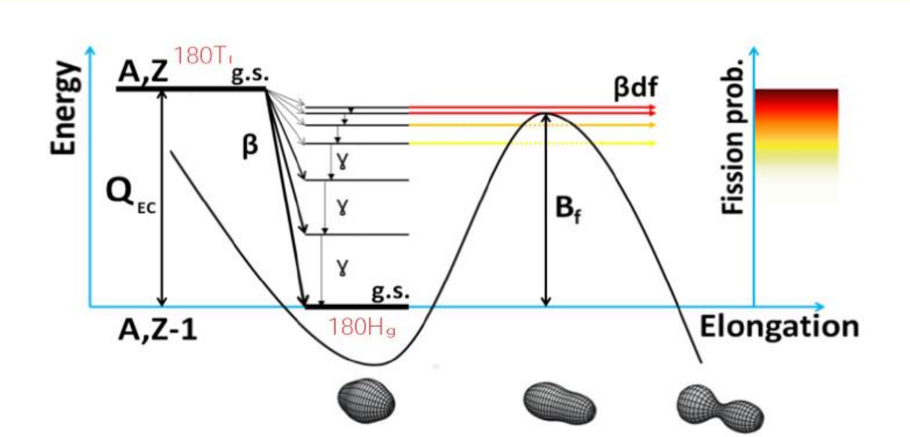

Potential surface in deformation and mass asymmetry

→ Role of shell effects at large deformation.

Virtual Photons and the Transition Strength

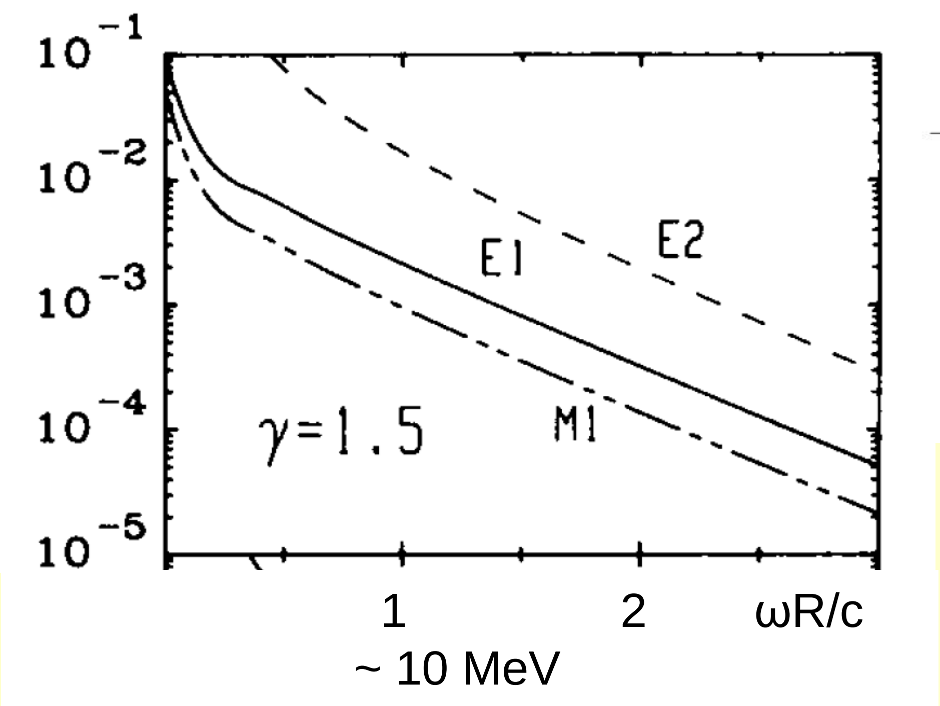

R is cutoff parameter ~ 10 fm

Nuclear Physics A442 (1985) 739–752
C.A. BERTULANI* and G. BAUR

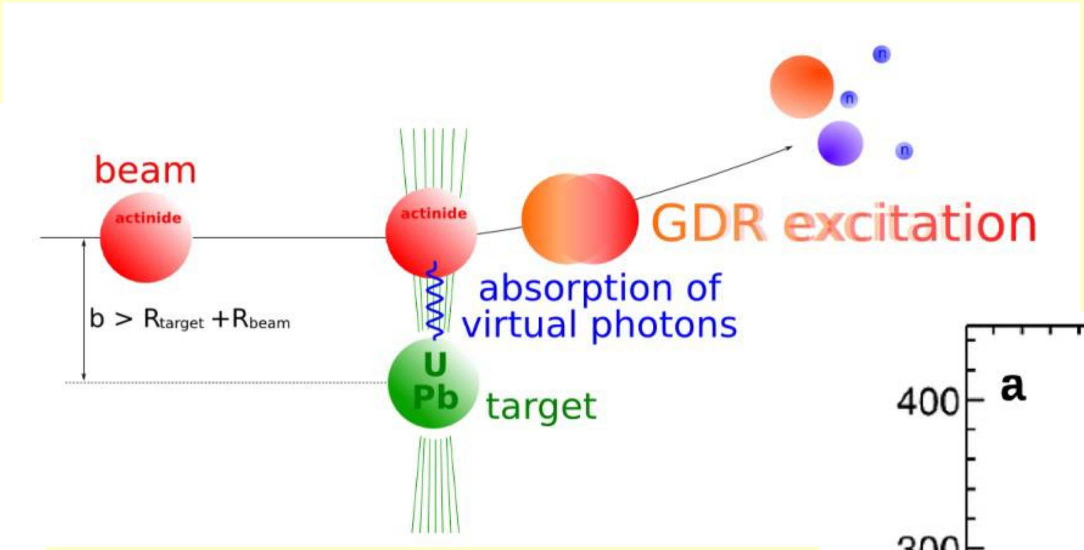

$$\sigma_c = \sum_f \int \sigma(\varepsilon)\rho_f(\varepsilon)\, d\varepsilon$$

dominated by GDR
for the E1 case

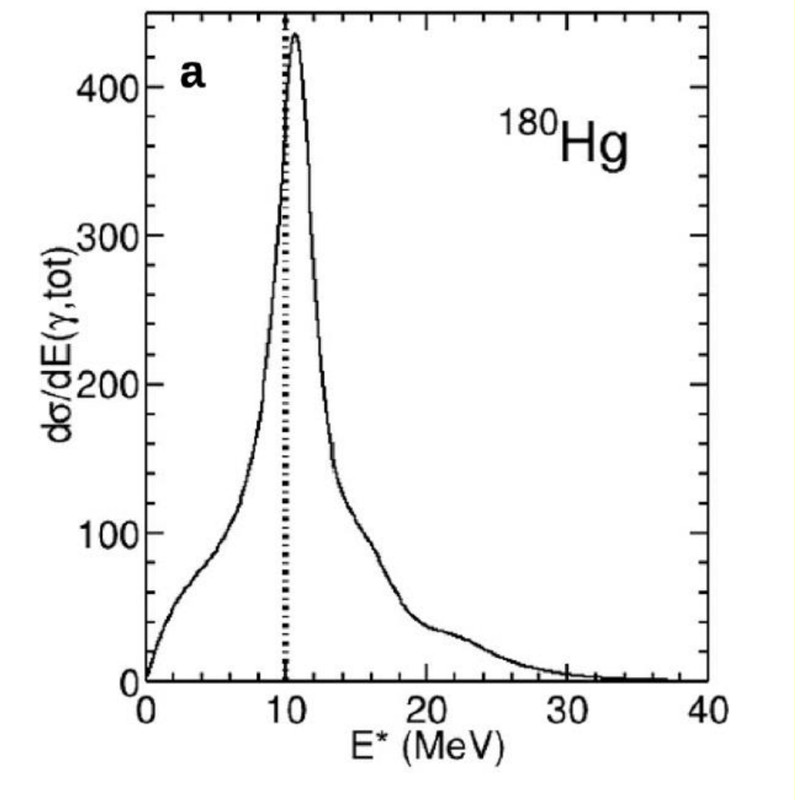

R3B Setup for Fission Experiments

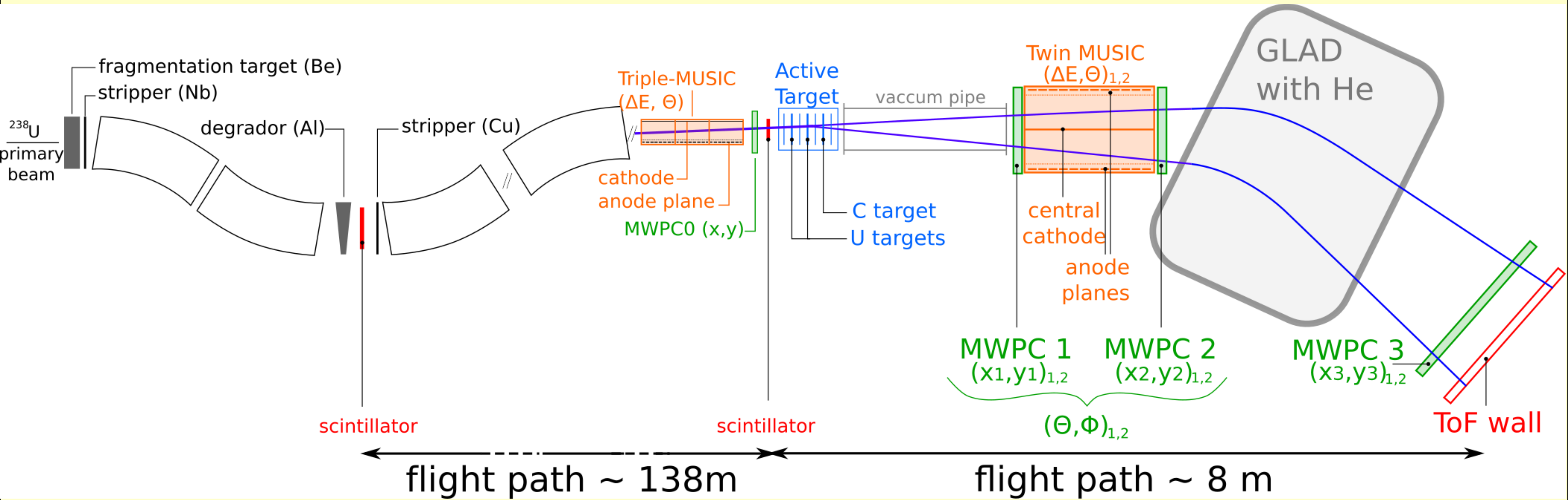

Four Settings Joint for the Incoming

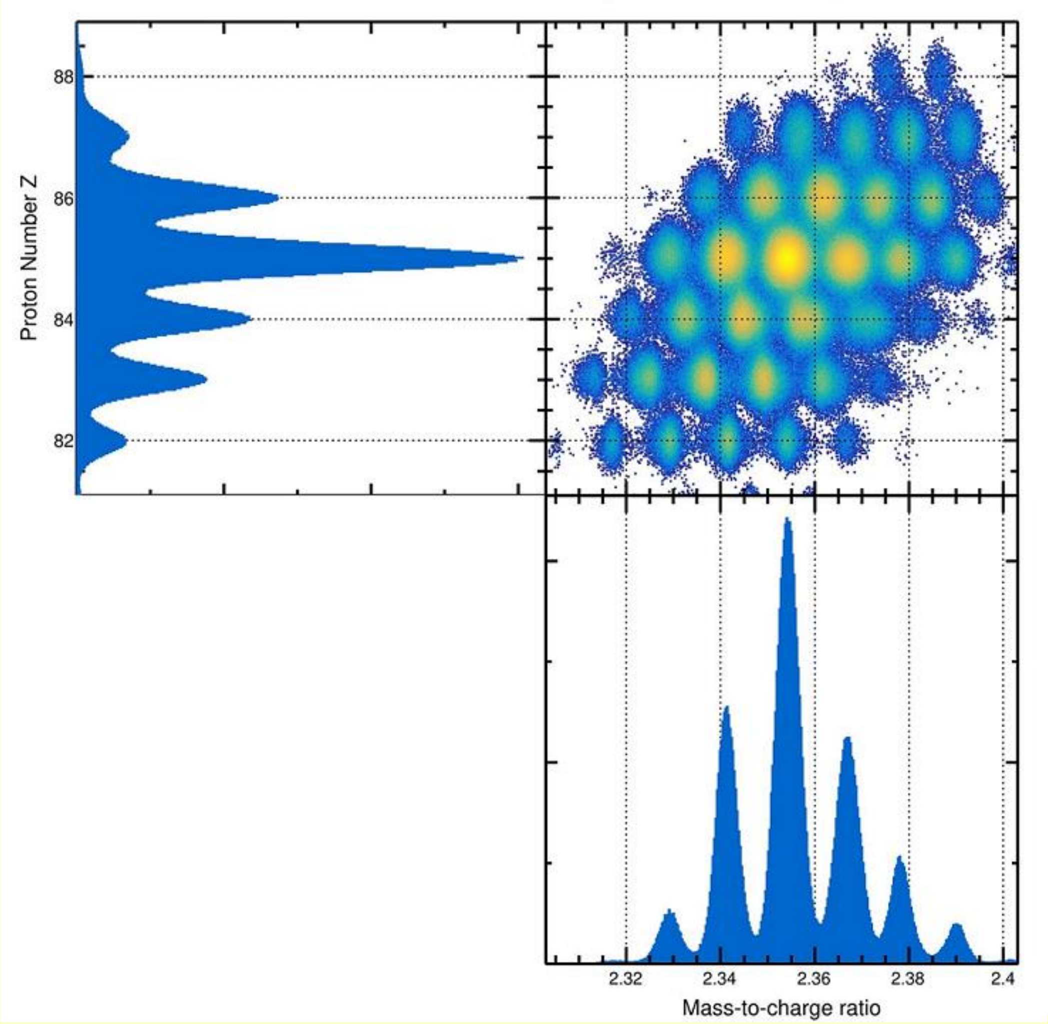

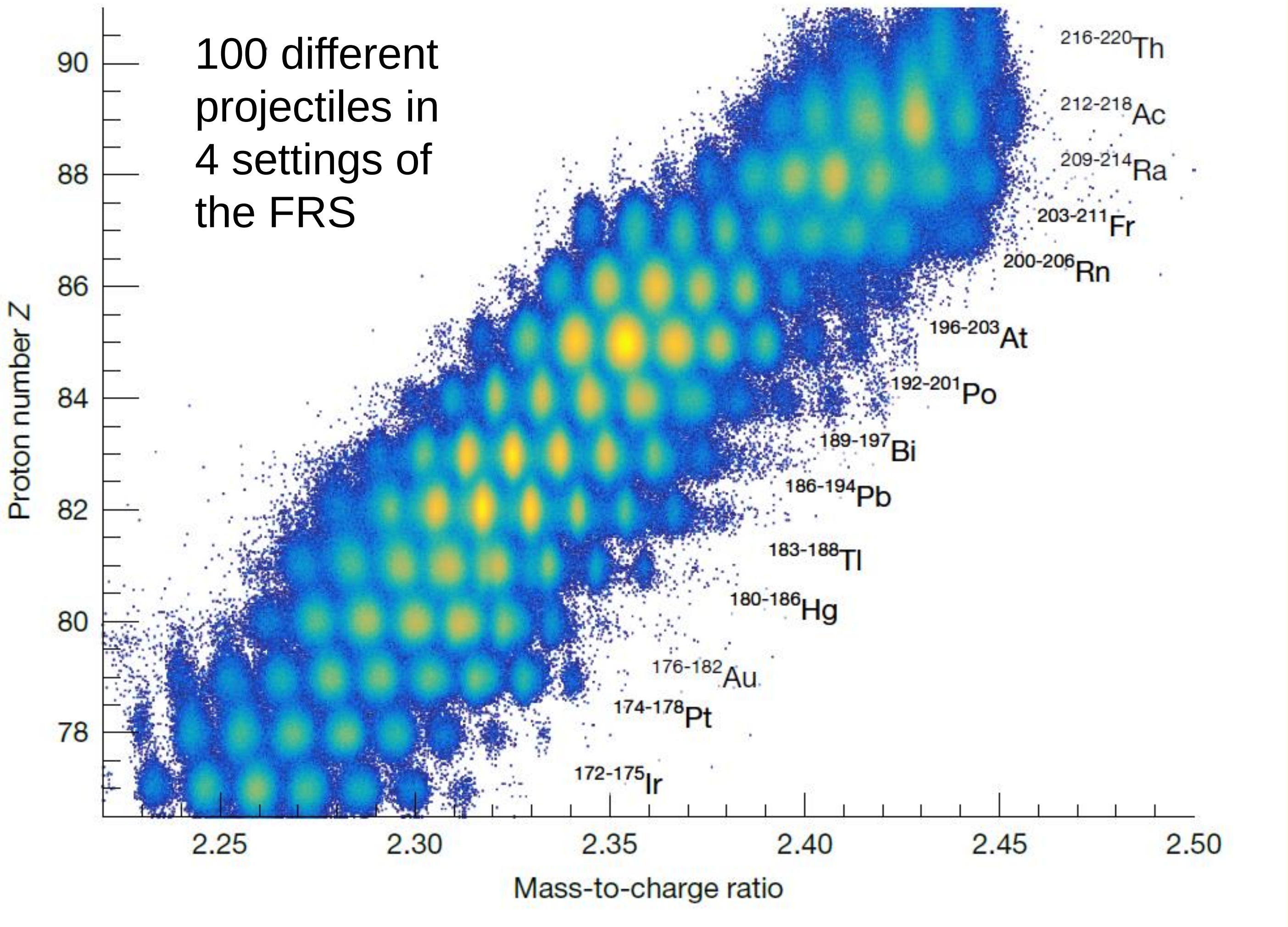

100 different projectiles in 4 settings of the FRS

Active Target

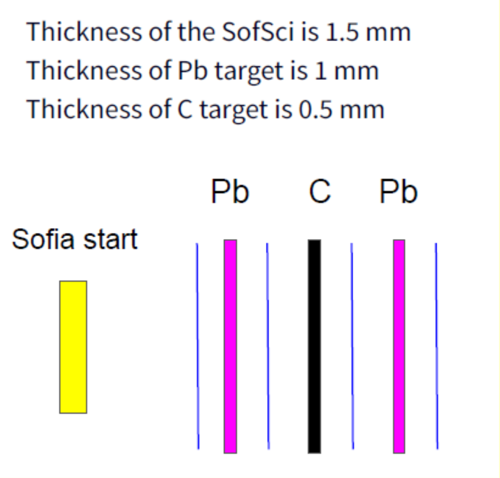

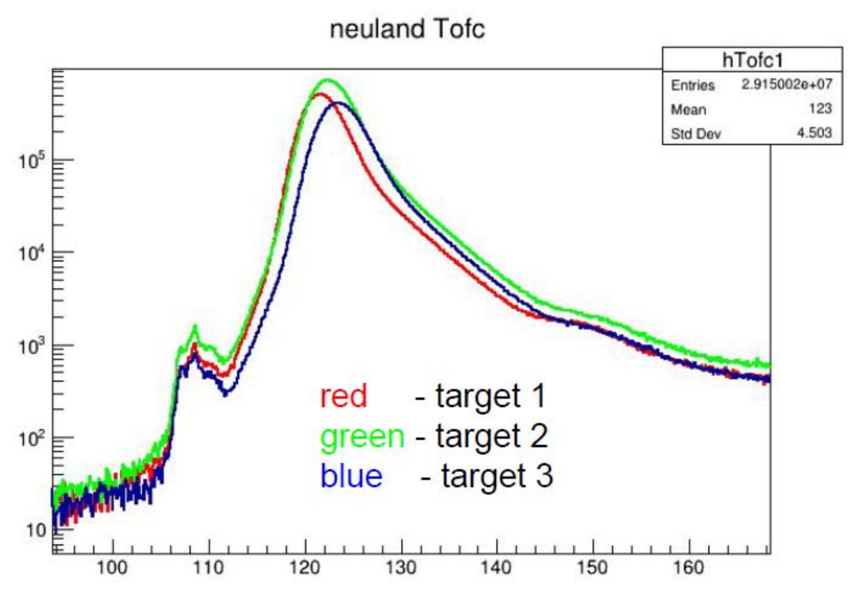

Separate Coulomb excitation from inelastic scattering

$Z_1^2 + Z_2^2 << (Z_1+Z_2)^2$

Kinematics of Fission Fragments

Fragments are in most cases well separated

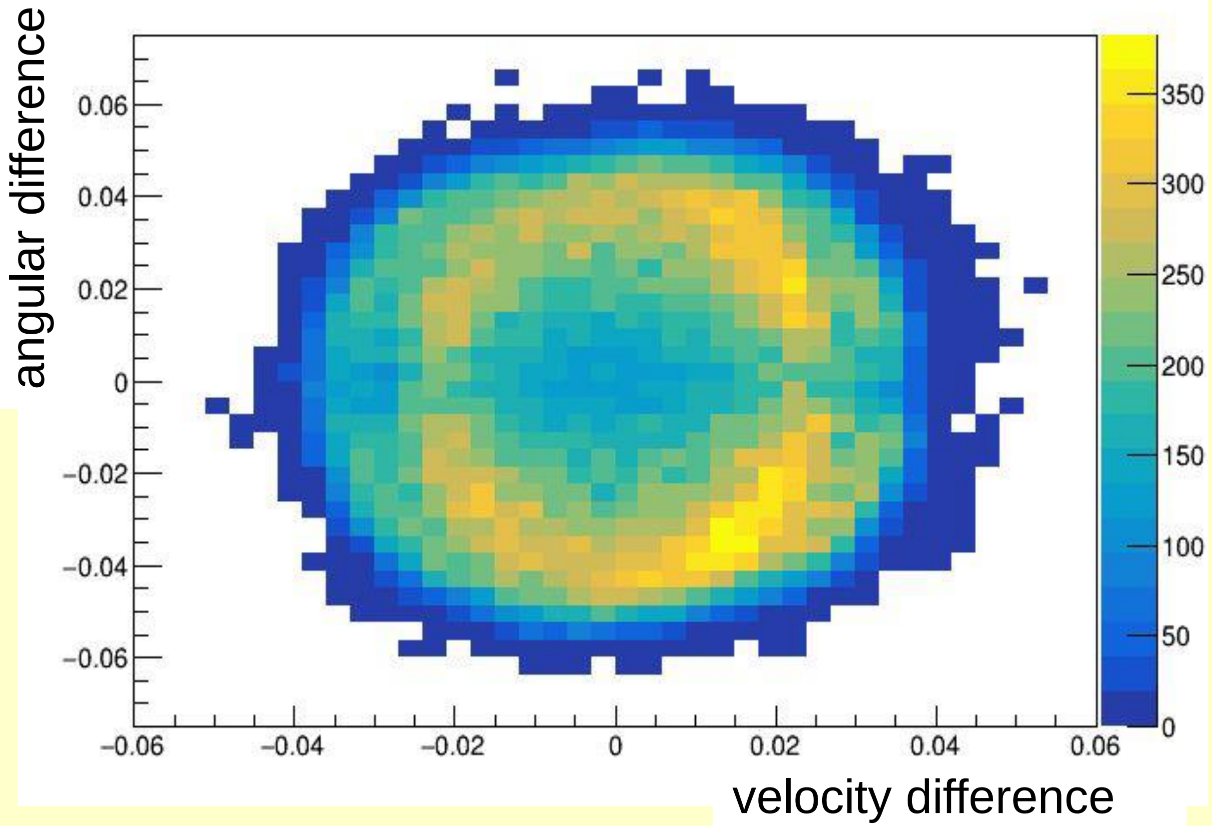

Back to back emission in the CM system allows for a clear separation

TWIN MUSIC

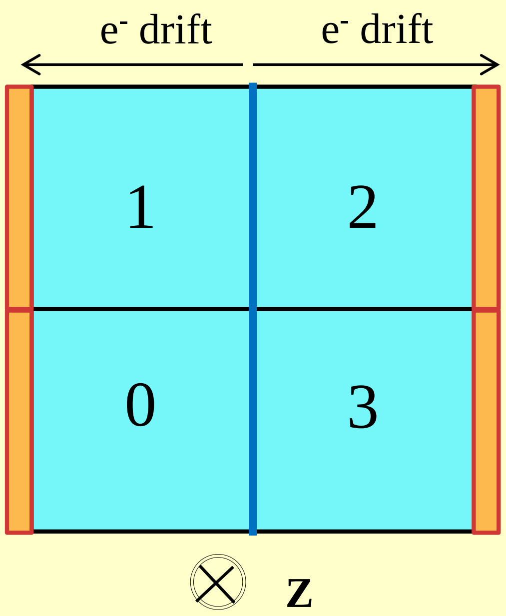

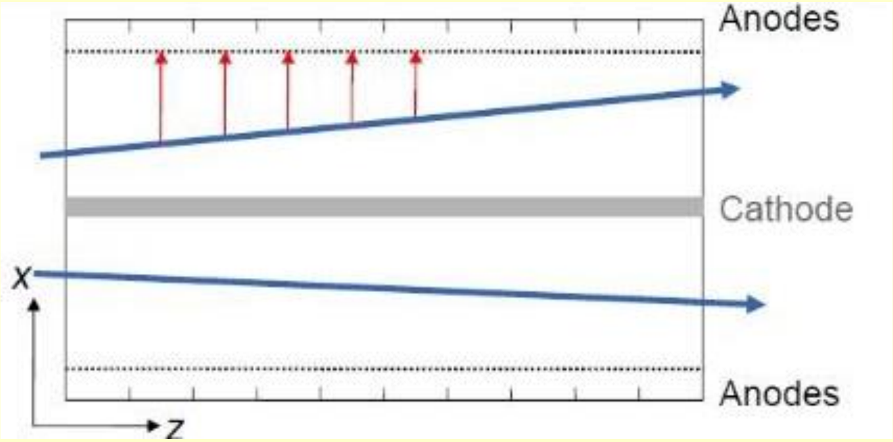

4 x 16 anodes read out

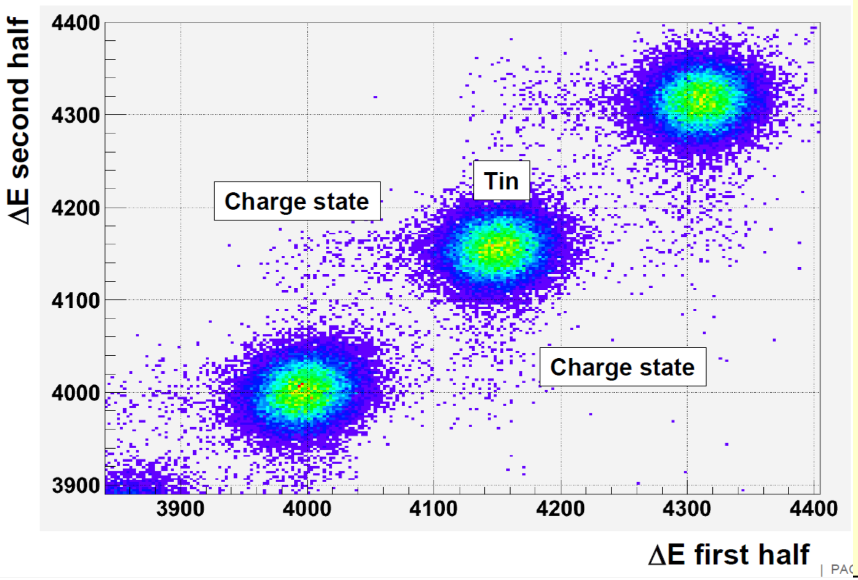

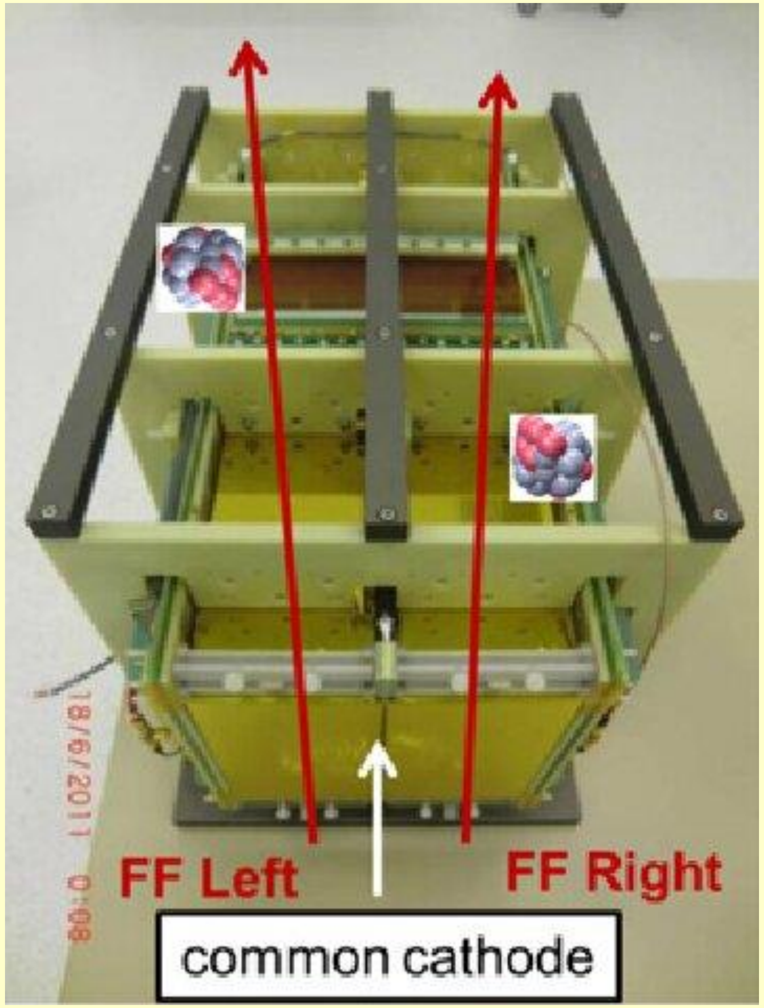

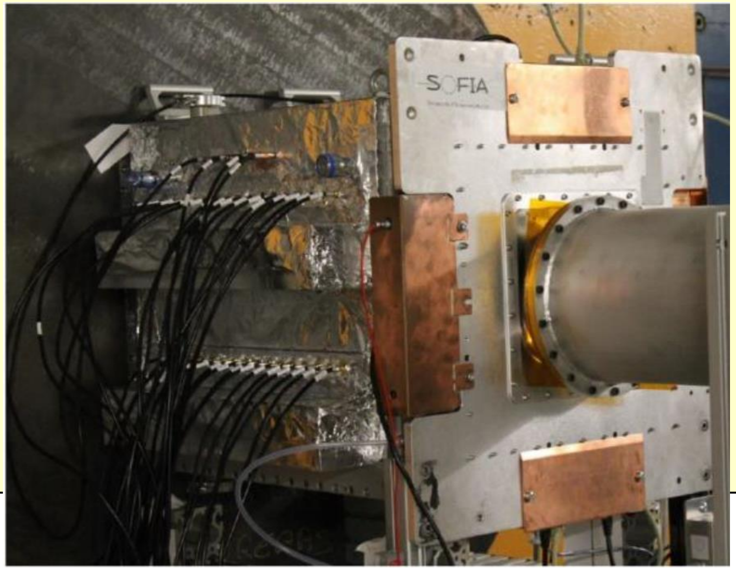

Charge Pattern ^{238}U

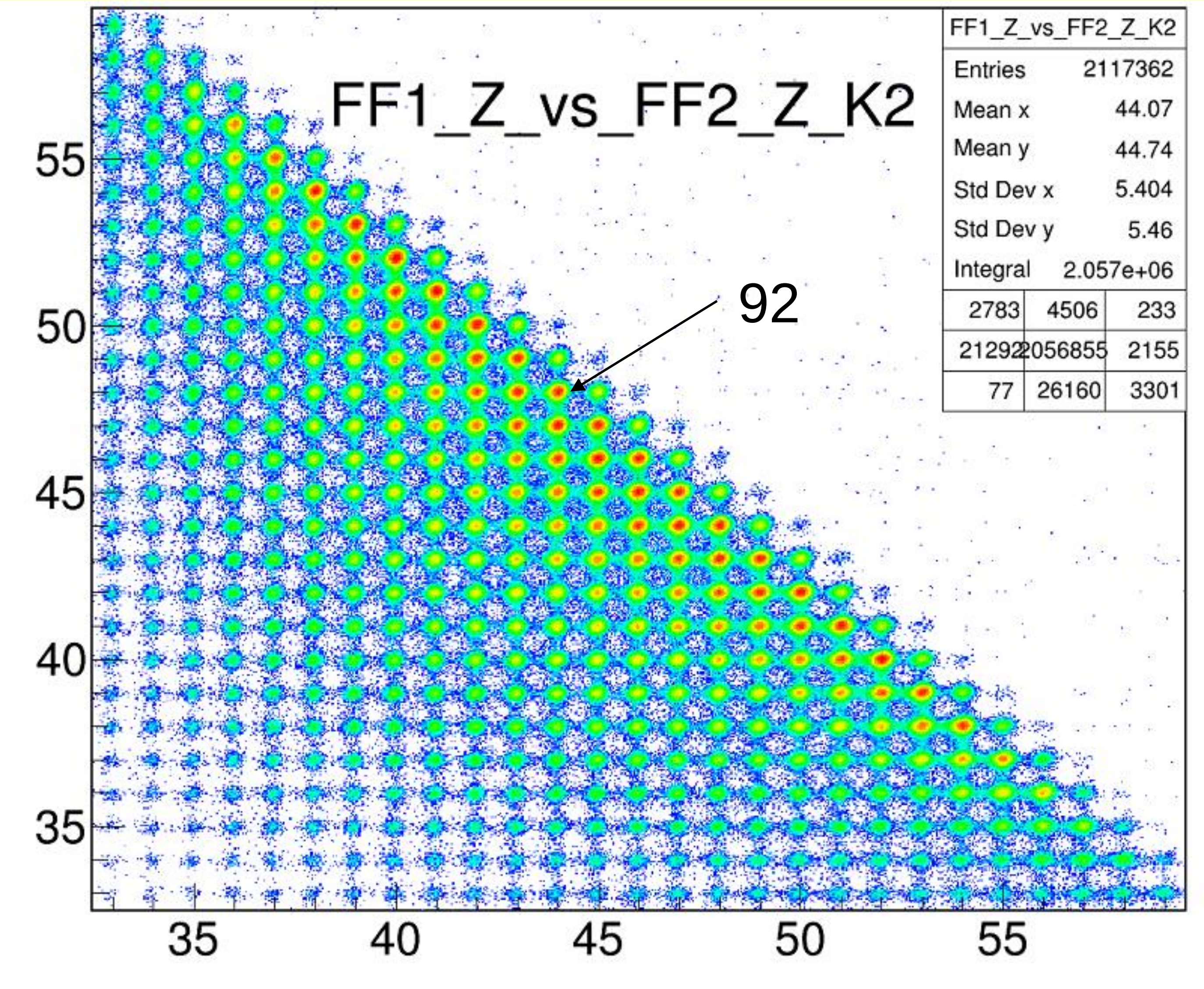

Calibration run with primary beam

Here selected:
Carbon target
Large E*

Different Charge Pattern

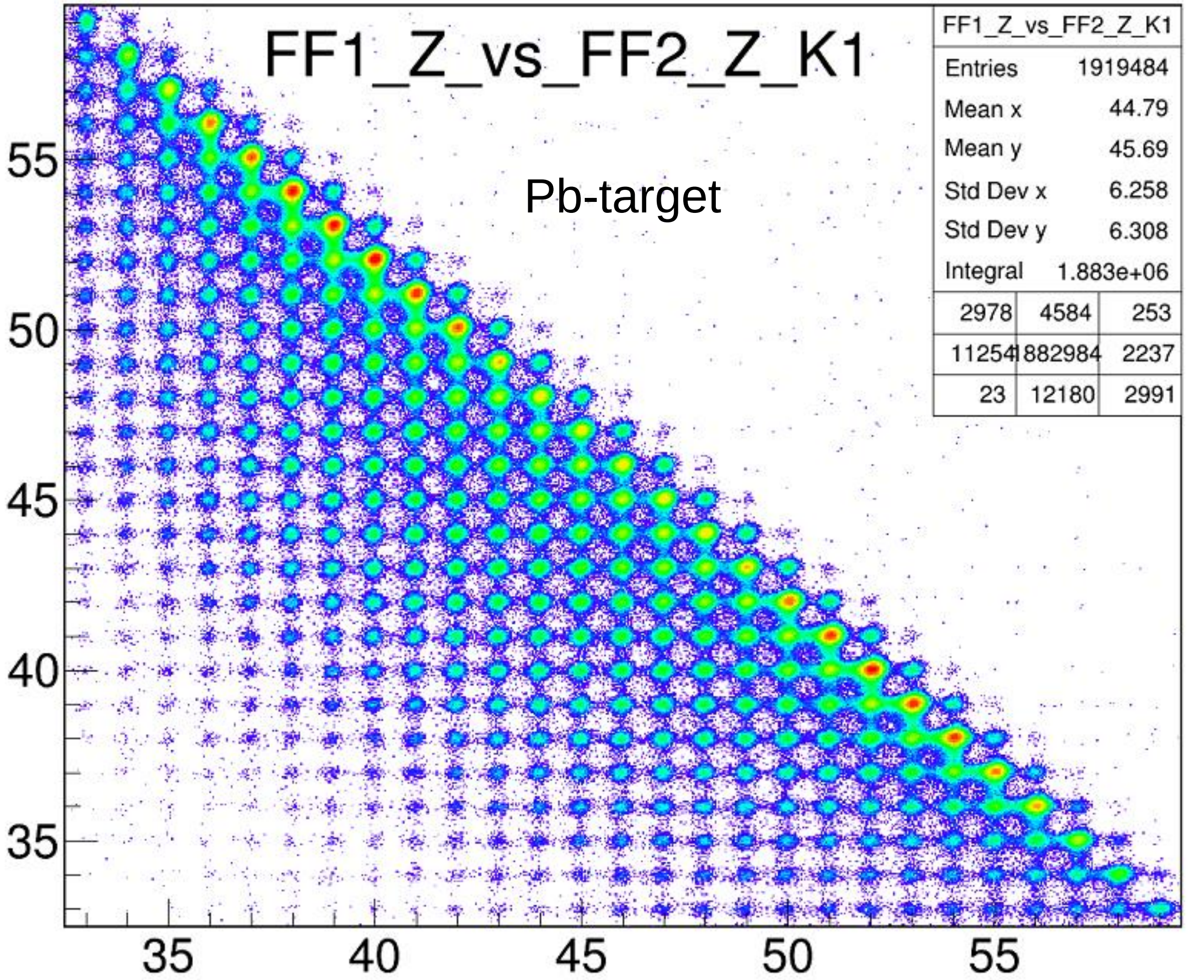

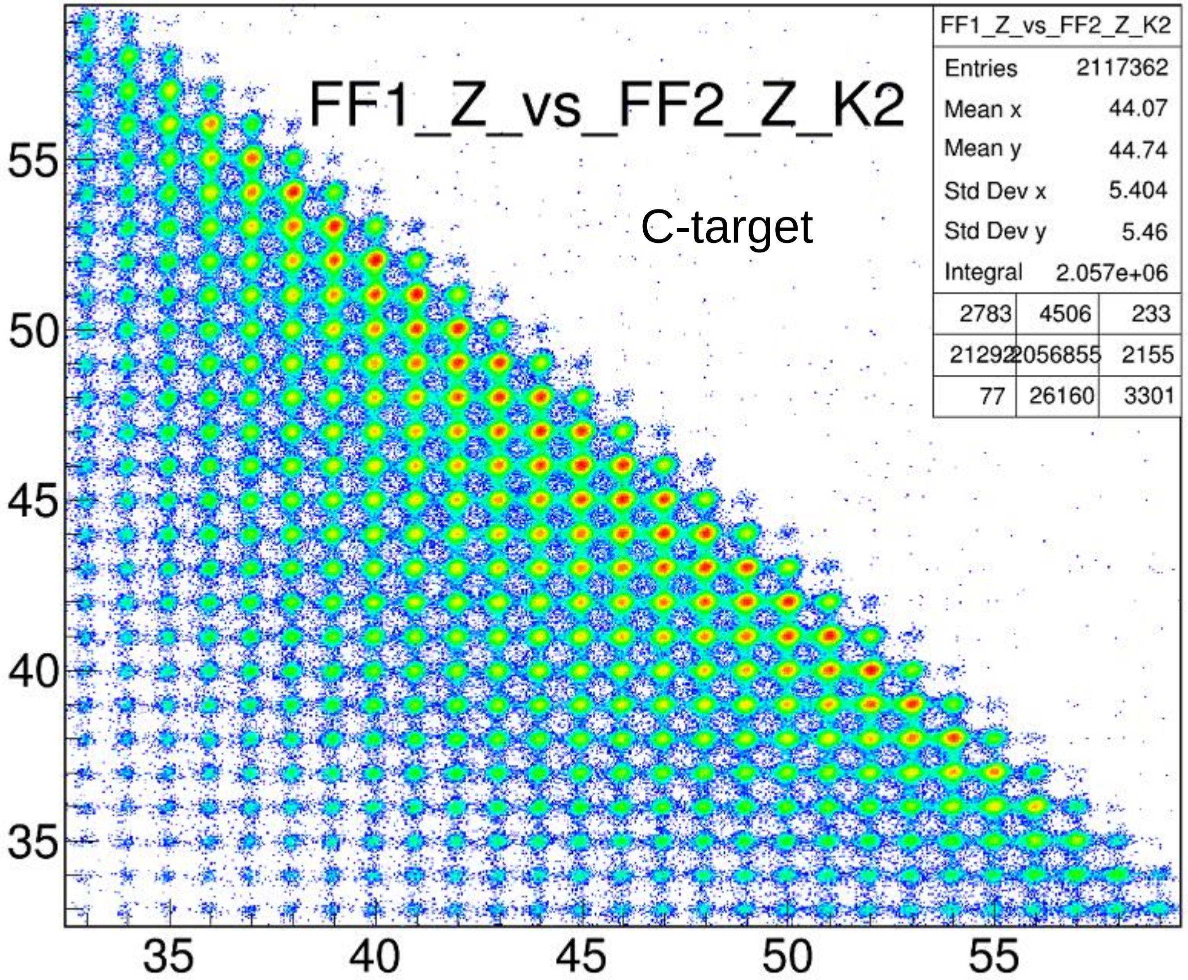

Charge Distributions 90 > Z > 84

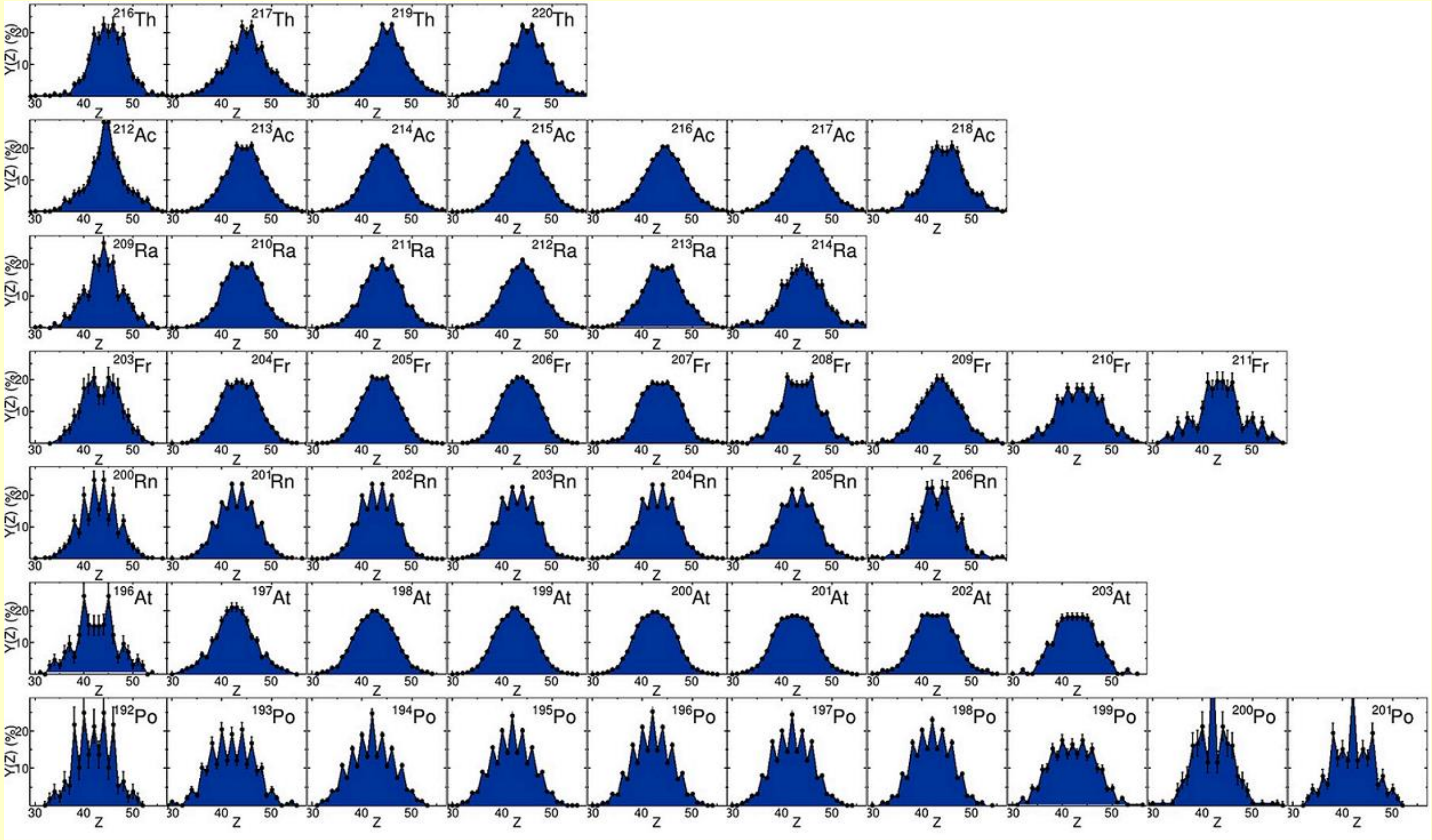

More odd-even

Charge Distributions 83 > Z > 77

Very distinct pattern

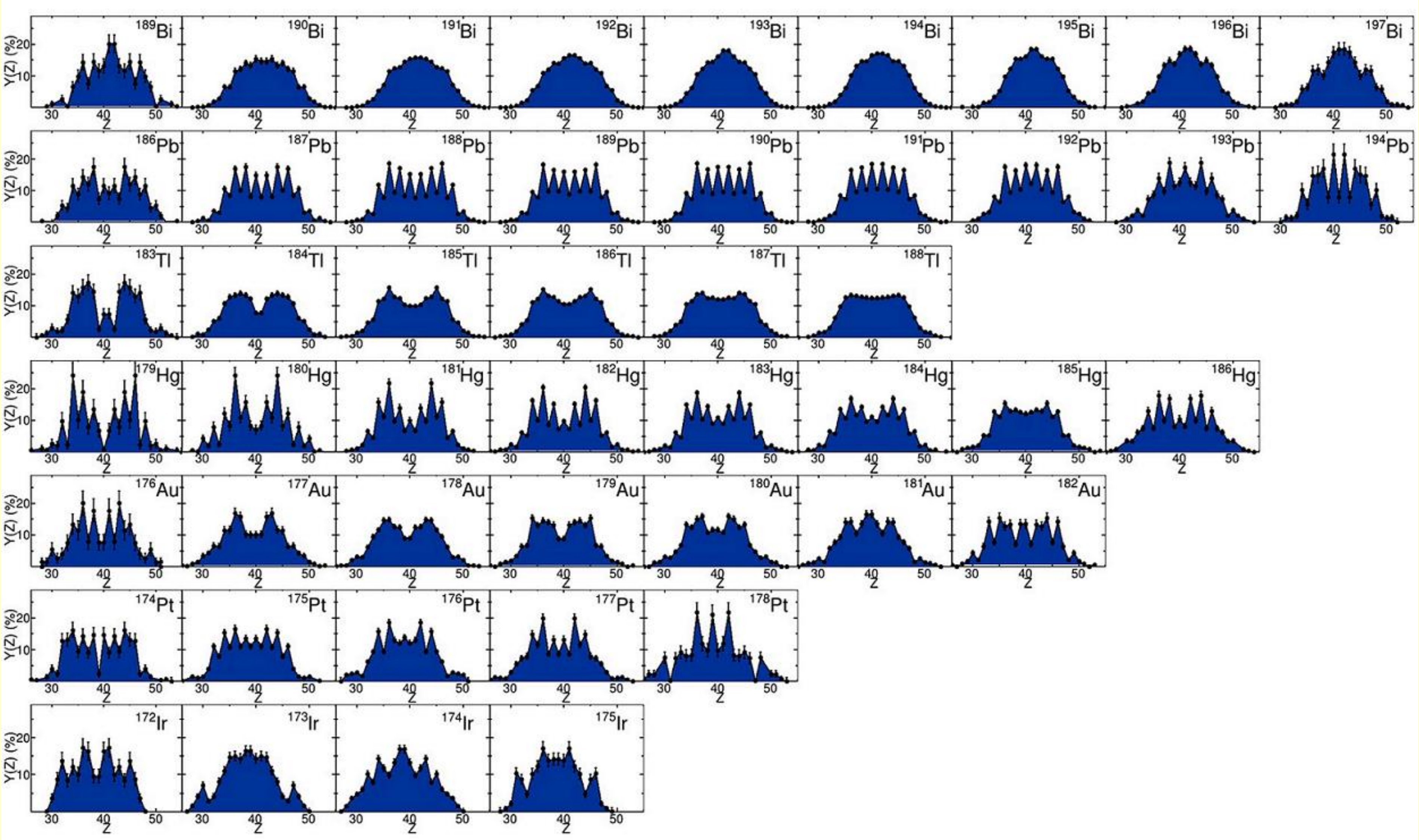

100 Different Fissioning Systems

Nucleus	Coulex ratio (%)	$\mathcal{A}_{exp}$	$\mathcal{A}_{GEF}$	$\mathcal{A}_{gauss}$	σ_Z	Z_L^{GEF}
^{172}Ir	44.7	0.27(12)	0.30	0.89	7.4	35
^{173}Ir	36.9	0.00(8)	0.27	0.99	6.3	36
^{174}Ir	33.9	0.00(6)	0.42	0.67	6.8	36
^{175}Ir	20.9	0.08(10)	0.22	0.51	6.6	36
^{174}Pt	69.9	0.39(11)	0.40	2.77	8.1	36
^{175}Pt	60.4	0.13(6)	0.43	1.01	7.2	36
^{176}Pt	43.3	0.15(5)	0.37	1.22	6.7	36
^{177}Pt	36.3	0.29(6)	0.38	1.41	7.0	36
^{178}Pt	47.5	0.05(16)	0.35	0.84	7.0	36
^{176}Au	76.3	0.33(17)	0.49	1.50	7.2	36
^{177}Au	75.4	0.36(6)	0.43	1.23	6.9	36
^{178}Au	69.4	0.33(4)	0.43	1.46	7.2	36
^{179}Au	56.8	0.23(5)	0.37	1.42	7.2	36
^{180}Au	45.8	0.23(4)	0.36	1.24	6.8	36
^{181}Au	35.5	0.00(6)	0.30	0.88	6.4	36
^{182}Au	28.7	0.09(9)	0.28	1.24	7.6	36
^{179}Hg	78.3	0.77(8)	0.40	5.06	9.8	36
^{180}Hg	83.3	0.56(7)	0.35	1.77	7.9	36
^{181}Hg	73.9	0.50(4)	0.43	1.86	8.0	36
^{182}Hg	68.0	0.44(2)	0.33	1.57	7.9	36
^{183}Hg	58.5	0.34(2)	0.39	1.36	7.6	36
^{184}Hg	47.9	0.28(3)	0.26	1.36	7.3	36
^{185}Hg	37.2	0.12(4)	0.26	1.06	6.9	36
^{186}Hg	29.0	0.32(6)	0.16	1.15	7.4	36
^{183}Tl	79.2	0.64(7)	0.28	4.59	8.3	36
^{184}Tl	80.6	0.37(3)	0.32	1.55	7.4	36
^{185}Tl	77.0	0.31(2)	0.30	1.43	7.5	36
^{186}Tl	71.4	0.25(2)	0.29	1.31	7.3	36
^{187}Tl	57.1	0.12(2)	0.24	1.11	7.0	36
^{188}Tl	46.1	0.06(2)	0.25	1.01	7.0	36
^{186}Pb	76.2	0.25(14)	0.12	1.35	7.7	36
^{187}Pb	84.1	0.16(5)	0.15	1.24	7.4	36
^{188}Pb	82.4	0.17(2)	0.12	1.19	7.7	36
^{189}Pb	79.6	0.10(1)	0.18	1.03	7.3	36
^{190}Pb	72.2	0.00(1)	0.16	0.94	7.2	38
^{191}Pb	61.4	0.00(2)	0.18	0.82	6.8	38
^{192}Pb	51.2	0.00(3)	0.13	0.81	6.9	38
^{193}Pb	32.4	0.00(9)	0.09	0.82	6.6	38
^{194}Pb	32.0	0.00(9)	0.07	0.80	6.9	38
^{189}Bi	78.5	0.00(14)	0	0.74	6.7	41
^{190}Bi	86.6	0.00(6)	0	0.77	6.3	41
^{191}Bi	83.4	0.00(3)	0	0.68	6.3	37
^{192}Bi	82.7	0.00(1)	0.04	0.67	6.1	38
^{193}Bi	78.1	0.00(1)	0.06	0.63	5.9	38
^{194}Bi	70.8	0.00(1)	0.06	0.72	6.0	38
^{195}Bi	59.7	0.00(2)	0.06	0.71	5.8	38
^{196}Bi	48.3	0.00(4)	0.05	0.76	5.9	38
^{197}Bi	51.3	0.00(10)	0.04	0.60	6.0	39

Nucleus	Coulex ratio (%)	$\mathcal{A}_{exp}$	$\mathcal{A}_{GEF}$	$\mathcal{A}_{gauss}$	σ_Z	Z_L^{GEF}
^{192}Po	79.6	0.07(22)	0	0.97	6.1	42
^{193}Po	83.9	0.04(9)	0	0.82	6.2	42
^{194}Po	85.6	0.00(3)	0	0.49	6.0	42
^{195}Po	84.1	0.00(2)	0	0.50	5.8	42
^{196}Po	80.7	0.00(2)	0	0.47	5.6	42
^{197}Po	74.2	0.00(2)	0	0.86	5.7	42
^{198}Po	63.4	0.00(3)	0	0.82	5.7	42
^{199}Po	52.8	0.05(8)	0	0.86	6.2	42
^{200}Po	57.3	0.00(2)	0	0.97	5.5	42
^{201}Po	70.4	0.00(1)	0	0.88	5.4	42
^{196}At	85.6	0.22(15)	0	0.23	6.0	42
^{197}At	81.3	0.00(6)	0	1.00	5.2	42
^{198}At	85.9	0.00(2)	0	0.95	5.3	42
^{199}At	84.5	0.00(1)	0	0.66	5.3	42
^{200}At	79.2	0.00(1)	0	0.78	5.4	42
^{201}At	68.6	0.00(1)	0	0.85	5.5	42
^{202}At	56.4	0.00(3)	0	0.73	5.4	42
^{203}At	45.7	0.00(6)	0	0.62	5.6	42
^{200}Rn	88.5	0.00(12)	0	0.43	5.5	42
^{201}Rn	87.7	0.00(3)	0	0.45	5.3	42
^{202}Rn	85.4	0.00(1)	0	0.93	5.3	42
^{203}Rn	79.9	0.00(1)	0	0.99	5.3	42
^{204}Rn	68.0	0.00(2)	0	0.92	5.3	42
^{205}Rn	57.7	0.00(3)	0	0.71	5.3	42
^{206}Rn	45.4	0.08(9)	0	1.00	5.3	42
^{203}Fr	93.0	0.14(14)	0	0.99	5.7	43
^{204}Fr	86.1	0.00(5)	0	0.90	5.4	43
^{205}Fr	84.5	0.00(3)	0	0.89	5.2	43
^{206}Fr	78.3	0.00(3)	0	0.80	5.3	43
^{207}Fr	68.3	0.00(3)	0	0.95	5.4	43
^{208}Fr	59.7	0.00(6)	0	0.45	5.4	43
^{209}Fr	50.3	0.00(6)	0	0.55	5.4	43
^{210}Fr	44.1	0.00(8)	0	0.16	5.9	43
^{211}Fr	32.6	0.00(14)	0	0.22	5.9	43
^{209}Ra	77.7	0.00(9)	0	0.52	5.1	44
^{210}Ra	75.0	0.00(3)	0	0.93	5.2	44
^{211}Ra	64.7	0.00(2)	0	0.83	5.2	44
^{212}Ra	57.1	0.00(2)	0	0.97	5.2	44
^{213}Ra	57.1	0.00(3)	0	0.17	5.4	44
^{214}Ra	48.5	0.00(9)	0	1.00	5.4	44
^{212}Ac	81.8	0.00(9)	0	0.31	4.7	44
^{213}Ac	76.0	0.00(4)	0	0.93	5.1	44
^{214}Ac	69.8	0.00(3)	0	0.44	5.2	44
^{215}Ac	64.7	0.00(2)	0	0.10	5.2	44
^{216}Ac	59.2	0.00(1)	0	0.52	5.3	44
^{217}Ac	67.7	0.00(3)	0	0.10	5.3	44
^{218}Ac	58.0	0.00(7)	0	0.12	5.4	44
^{216}Th	81.1	0.00(10)	0	0.11	5.0	44
^{217}Th	79.9	0.00(8)	0	0.54	5.3	44
^{219}Th	81.9	0.00(2)	0	0.51	5.1	44
^{220}Th	79.8	0.00(4)	0	0.11	5.1	44

Nucleus	B_f (MeV)	$\overline{E^*} - B_f$ (MeV)	σ_{E*} (MeV)	Second chance fission (%)
^{172}Ir	13.1	9.6	6.2	2.9
^{173}Ir	13.4	9.5	7.7	3.1
^{174}Ir	13.7	9.6	5.9	6.1
^{175}Ir	14.1	9.2	7.3	6.6
^{174}Pt	11.8	9.2	6.8	3.3
^{175}Pt	11.7	7.9	6.4	4.3
^{176}Pt	12.5	10.4	6.8	5.8
^{177}Pt	12.7	10.5	7.7	9.2
^{178}Pt	13.3	11.8	7.8	10.9
^{176}Au	10.2	5.6	5.5	2.3
^{177}Au	10.6	6.9	5.6	4.9
^{178}Au	10.9	6.9	5.9	7.3
^{179}Au	11.2	8.3	6.2	9.0
^{180}Au	11.8	8.6	6.5	11.4
^{181}Au	12.1	9.9	7.0	13.2
^{182}Au	12.8	9.8	7.0	14.1
^{179}Hg	9.3	5.1	4.8	2.9
^{180}Hg	10.0	7.4	5.5	6.5
^{181}Hg	10.1	6.2	5.4	6.8
^{182}Hg	10.7	8.5	5.8	10.4
^{183}Hg	11.0	7.8	6.1	12.8
^{184}Hg	11.6	10.0	6.7	13.7
^{185}Hg	11.8	9.3	6.9	15.5
^{186}Hg	12.7	11.7	7.1	14.7
^{183}Tl	9.3	6.1	4.8	6.3
^{184}Tl	9.3	5.6	4.9	8.1
^{185}Tl	10.1	6.4	5.2	11.4
^{186}Tl	10.3	6.6	5.7	13.3
^{187}Tl	11.1	7.3	6.1	15.4
^{188}Tl	11.5	7.8	6.4	17.1
^{186}Pb	8.6	6.3	4.7	5.7
^{187}Pb	8.7	5.6	4.4	6.4
^{188}Pb	9.5	6.9	5.3	12.9
^{189}Pb	9.8	5.9	5.1	13.0
^{190}Pb	10.6	7.9	6.1	17.7
^{191}Pb	11.0	7.3	6.2	20.2
^{192}Pb	12.0	9.8	6.9	17.8
^{193}Pb	12.5	10.3	7.0	20.3
^{194}Pb	13.5	12.8	6.8	12.1
^{189}Bi	7.4	5.9	4.1	3.0
^{190}Bi	7.9	5.3	4.2	5.2
^{191}Bi	8.6	5.7	4.4	9.1
^{192}Bi	9.1	5.5	4.7	12.7
^{193}Bi	9.9	6.3	5.2	16.9
^{194}Bi	10.7	6.4	5.8	19.3
^{195}Bi	11.4	8.4	6.7	20.6
^{196}Bi	12.3	9.4	6.8	19.3
^{197}Bi	13.1	11.6	6.5	15.3

$$\mathcal{A} = 1 - \frac{Y(Z_{\rm sym}) + \frac{Y(Z_{\rm sym}-1)+Y(Z_{\rm sym}+1)}{2}}{Y(Z_{\rm max}) + \frac{Y(Z_{\rm max}-1)+Y(Z_{\rm max}+1)}{2}}$$

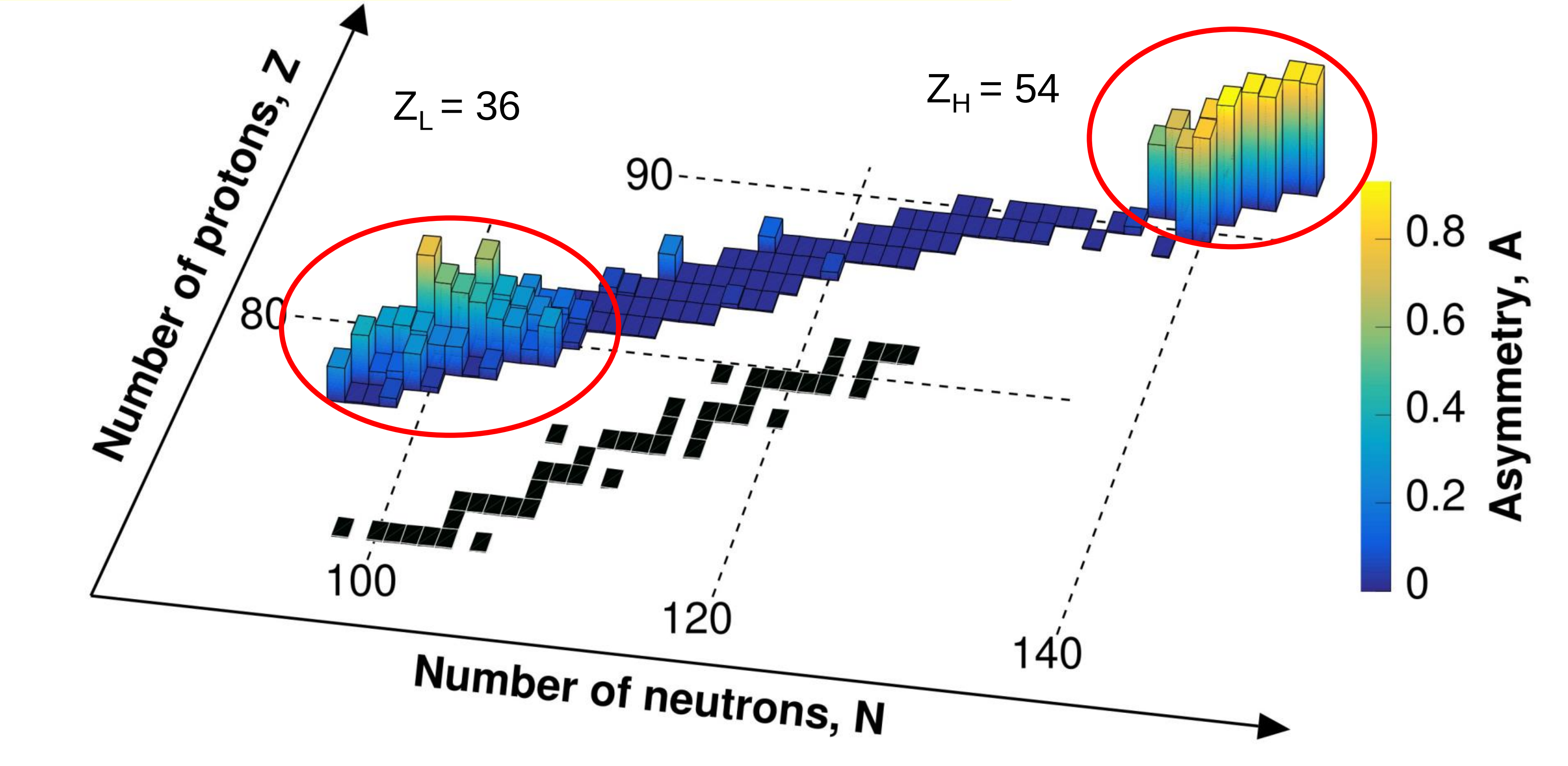

averaging the odd – even effect

Z-axis is color coded asymmetry parameter A

Influence of the Protons.

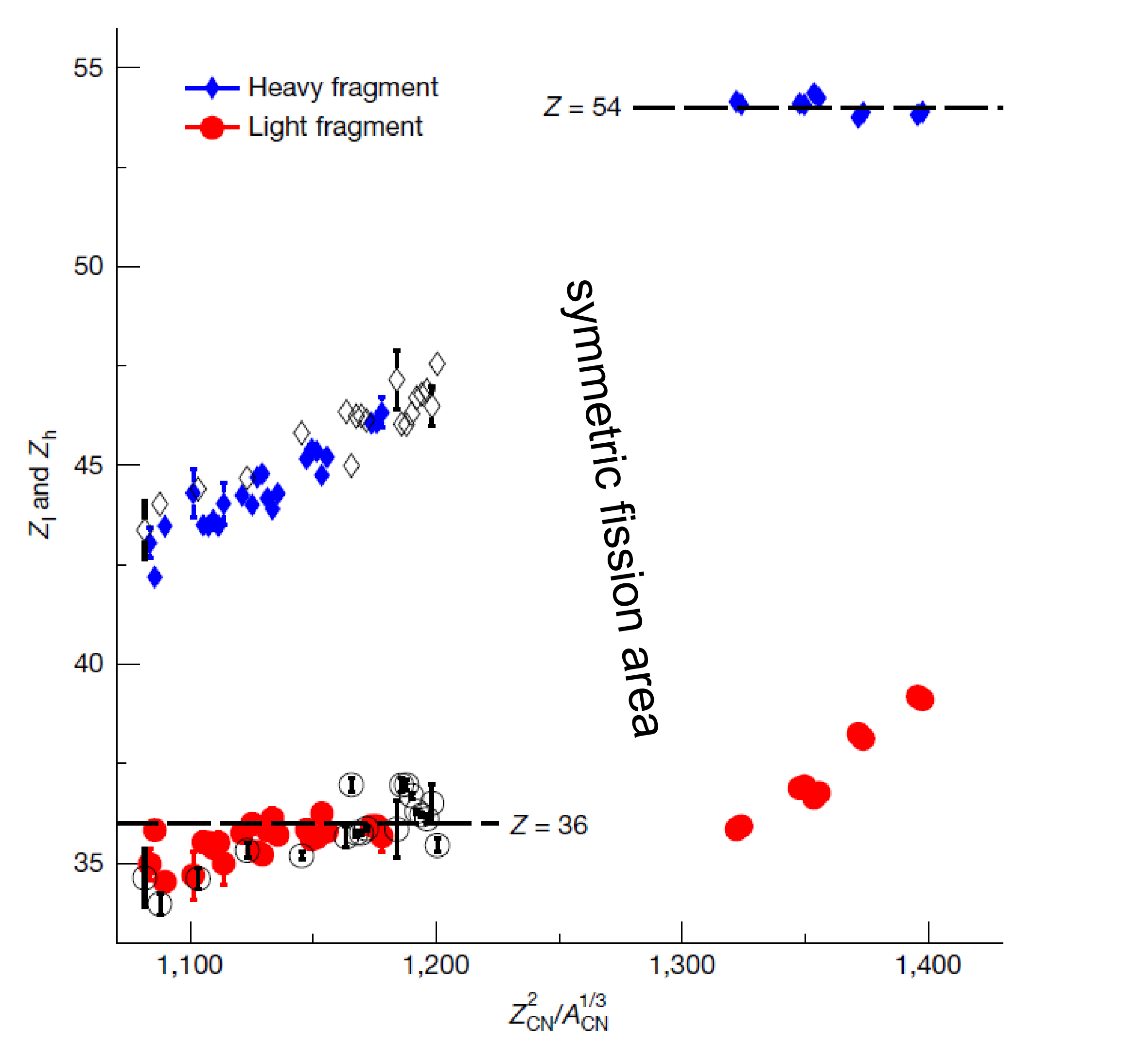

"Why is the influence of the protons so dominant in the sharing of nucleons in fission?", "Is the neutron subsystem strongly disturbed by the neck, while the protons are pushed away into the fragments by the Coulomb repulsion allowing specific stabilized configurations to manifest?".

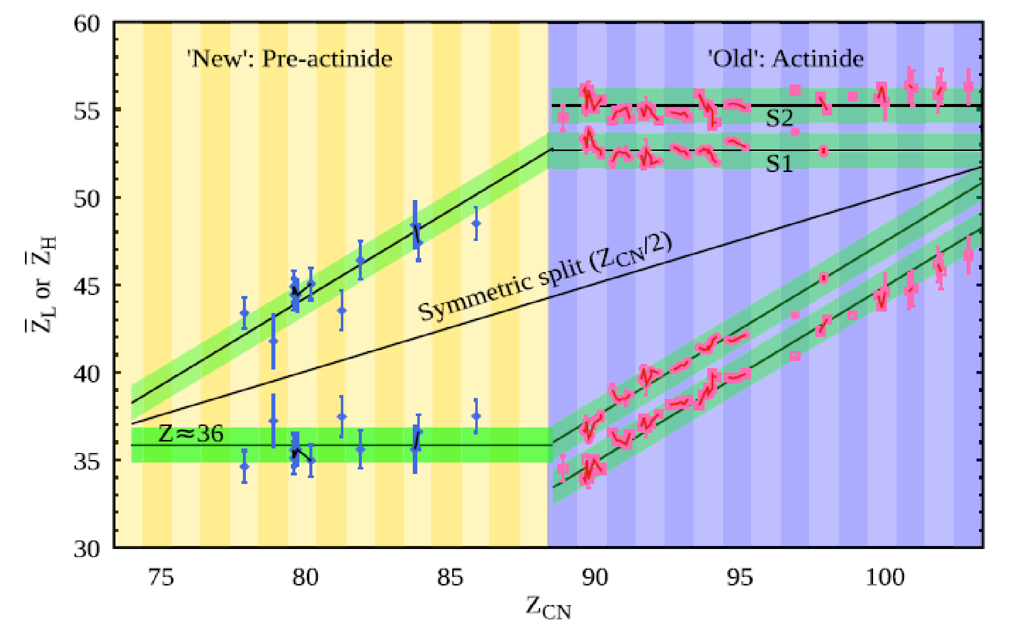

$A_H = 144$
$A_H = 140$

K. Mahata *et al.* Phys. Lett. B **825**, 136859 (2022)

Conclusion

- Measurement of fission charge yields of 100 neutron-deficient nuclei through Coulomb excitation.

✓ We delineate the boundaries of the new island of asymmetric fission.
✓ Direct experimental evidence of proton-shell stabilization at Z=36 in this new asymmetric split.
✓ Asymmetric fission driven by light fragment !
✓ Remarkable data set to test and constrain theoretical models.

Large scale microscopic calculations (HFB3 with the D1S Gogny interaction)
(N. Dubray, N. Pillet, D. Regnier, R. Bernard)
✓ Challenging calculations in this neutron-deficient region.

Article

An asymmetric fission island driven by shell effects in light fragments

https://doi.org/10.1038/s41586-025-08882-7

Received: 4 October 2024

Accepted: 11 March 2025

Published online: 30 April 2025

Check for updates

P. Morfouace[1,2]✉, J. Taieb[1,2], A. Chatillon[1,2], L. Audouin[3], G. Blanchon[1,2], R. N. Bernard[4], N. Dubray[1,2], N. Pillet[1,2], D. Regnier[1,2], H. Alvarez-Pol[5], F. Amjad[6], P. André[7], G. Authelet[7], L. Atar[8], T. Aumann[6,8,9], J. Benlliure[10], K. Boretzky[6], L. Bott[11], T. Brecelj[12], C. Caesar[6], P. Carpentier[1], E. Casarejos[13], J. Cederkäll[14], A. Corsi[7], D. Cortina-Gil[10], A. Cvetinović[12], E. De Filippo[15], T. Dickel[6,16], M. Feijoo[5], L. M. Fonseca[6,8,9,17], D. Galaviz[18,19], G. García-Jiménez[5], I. Gasparic[20], E. I. Geraci[15,21], R. Gernhäuser[22], B. Gnoffo[15,21], K. Göbel[11], A. Graña-González[5], E. Haettner[6], A.-L. Hartig[8], M. Heil[6], A. Heinz[23], T. Hensel[24], M. Holl[23], C. Hornung[6], A. Horvat[8], A. Jedele[6,8], D. Jelavic Malenica[20], T. Jenegger[22], L. Ji[8,9], H. T. Johansson[23], B. Jonson[23], B. Jurado[25], N. Kalantar-Nayestanaki[26], E. Kazantseva[6], A. Kelic-Heil[6], O. A. Kiselev[6], P. Klenze[22], R. Knöbel[6], D. Körper[6], D. Kostyleva[6], T. Kröll[8,9], N. Kuzminchuk[6], B. Laurent[1,2], I. Lihtar[20], Yu. A. Litvinov[6,9], B. Löher[6], N. S. Martorana[15], B. Mauss[1,2], S. Murillo Morales[27], D. Mücher[28,29], I. Mukha[6], E. Nacher[10], A. Obertelli[8,9], E. V. Pagano[30], V. Panin[6], J. Park[31], S. Paschalis[27], M. Petri[27], S. Pietri[6], S. Pirrone[15], G. Politi[15,21], L. Ponnath[8,9], A. Revel[7], H.-B. Rhee[8], J. L. Rodríguez-Sánchez[5,32], L. Rose[27], D. Rossi[6,8], P. Roy[6], P. Russotto[30], C. Scheidenberger[6,9,16], H. Scheit[8], H. Simon[6], S. Storck-Dutine[8], A. Stott[27], Y. L. Sun[8], C. Sürder[8,9], Y. K. Tanaka[6], R. Taniuchi[27], O. Tengblad[33], I. Tisma[12], H. T. Törnqvist[6,8], M. Trimarchi[15,34], S. Velardita[8], J. Vesic[12], B. Voss[6], F. Wamers[6], H. Weick[6], F. Wienholtz[8], J. Zhao[6] & M. Zhukov[23]

Outlook if three is time?

The Methods: Missing Mass in (p,2p)

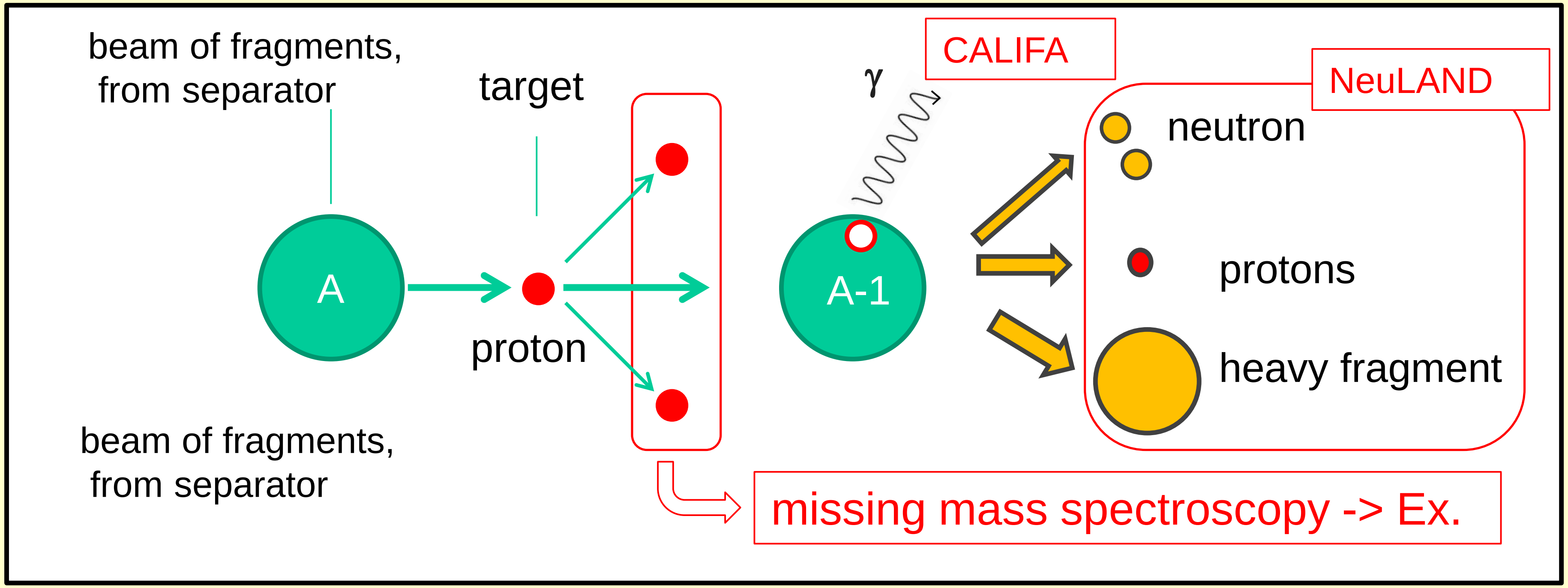

with courtesy of M. Sasano

$$\begin{pmatrix} E_A \\ \vec{p}_A \end{pmatrix} + \begin{pmatrix} m_p \\ 0 \end{pmatrix} = \begin{pmatrix} E_{p1} \\ \vec{p}_{p1} \end{pmatrix} + \begin{pmatrix} E_{p2} \\ \vec{p}_{p2} \end{pmatrix} + \begin{pmatrix} E \\ \vec{p} \end{pmatrix}$$

$$M^* = \sqrt{E^2 - \overrightarrow{p}^2} - M_{A-1} = \sqrt{\left(E_A + m_p - E_{p1} - E_{p2}\right)^2 - \left|\vec{p}_A - \vec{p}_{p1} - \vec{p}_{p2}\right|^2}$$

Angular Correlations of the Protons from (p,2p) Reactions

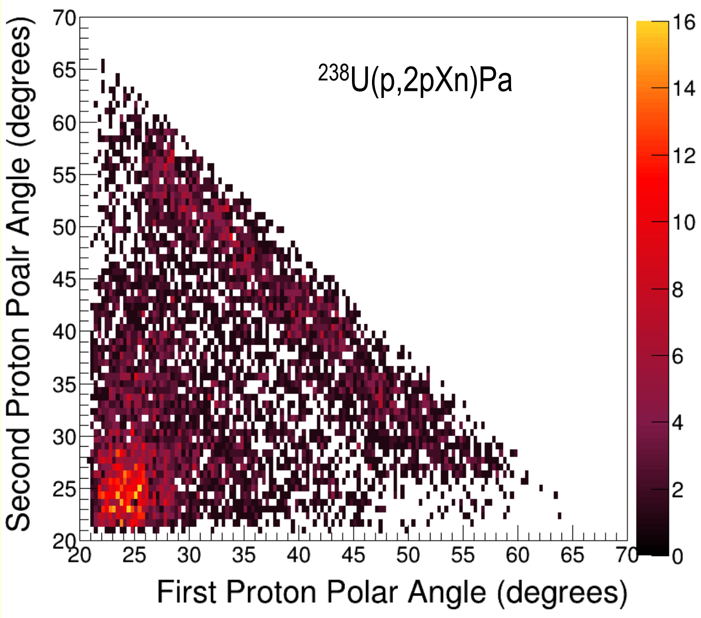

Low excitation energy,
No fission,
Protactinium in the exit channel

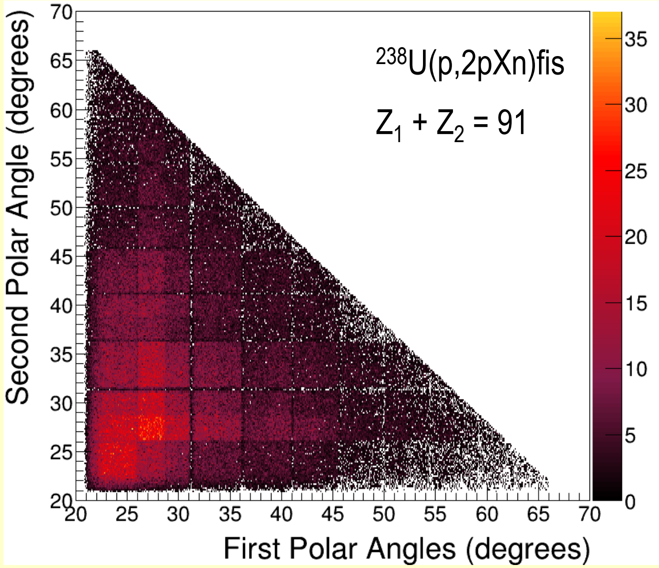

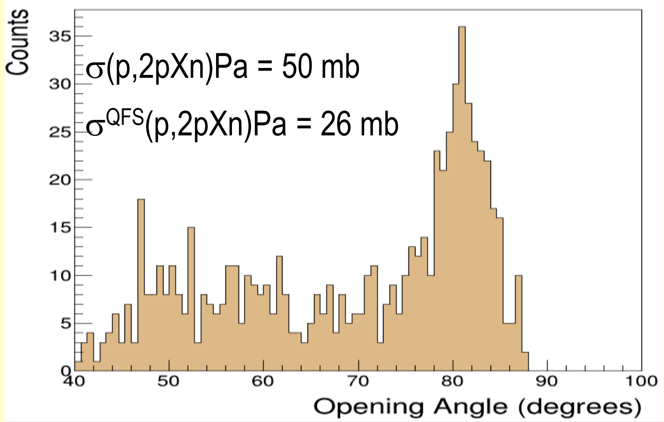

High excitation energy,
Fission,
2 heavy ions in the exit channel

First evidence for QFS-induced fission.

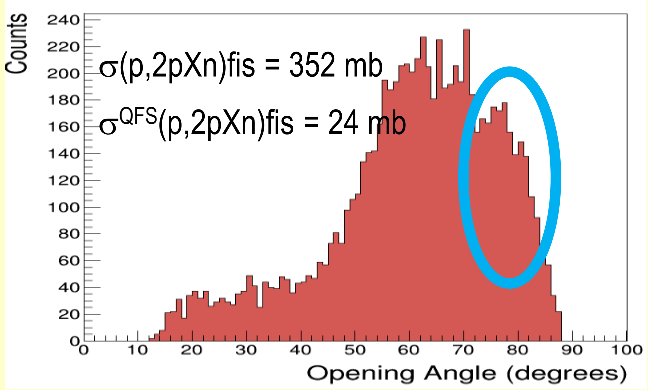

Credits to José Benlliure

28

Evolution of the charge distribution of fission fragments from $^{238}U(p,2p)$

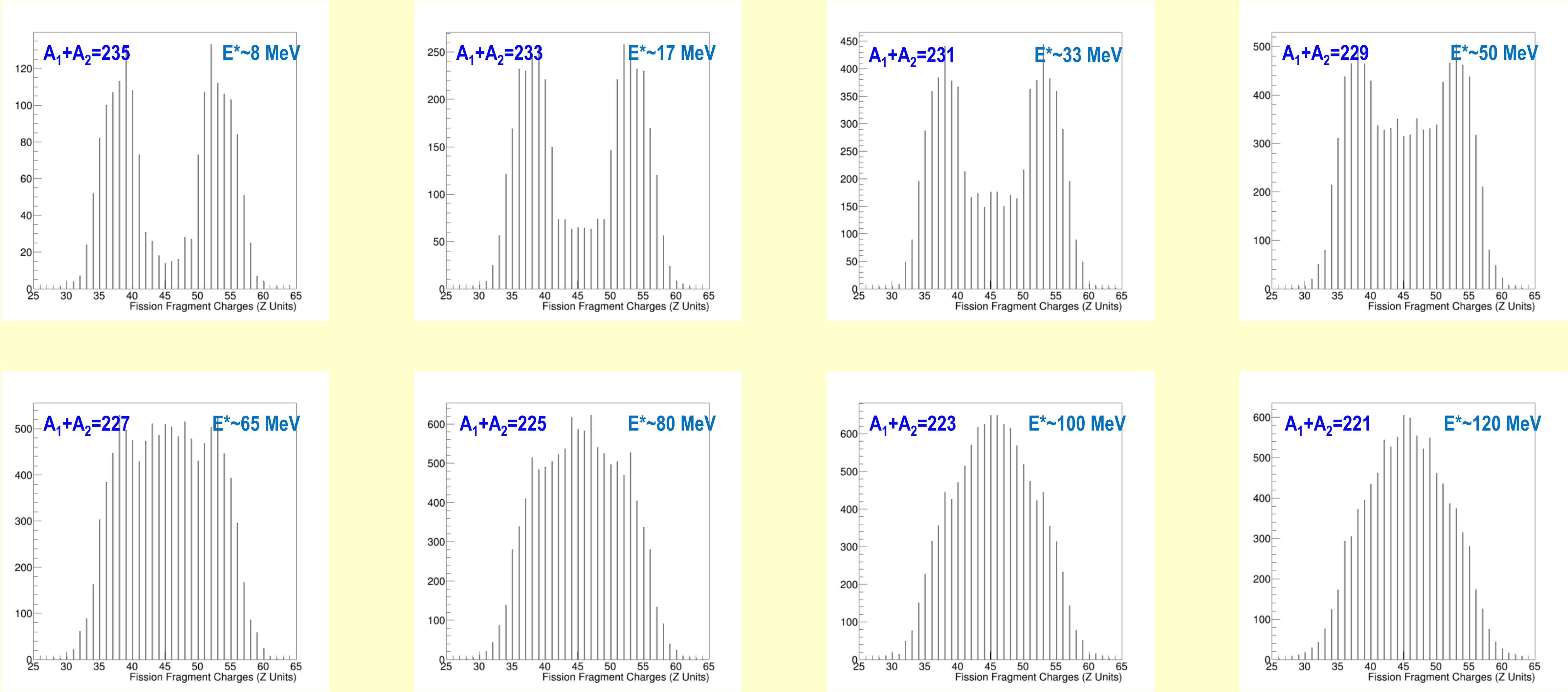

QFS Identification with CALIFA

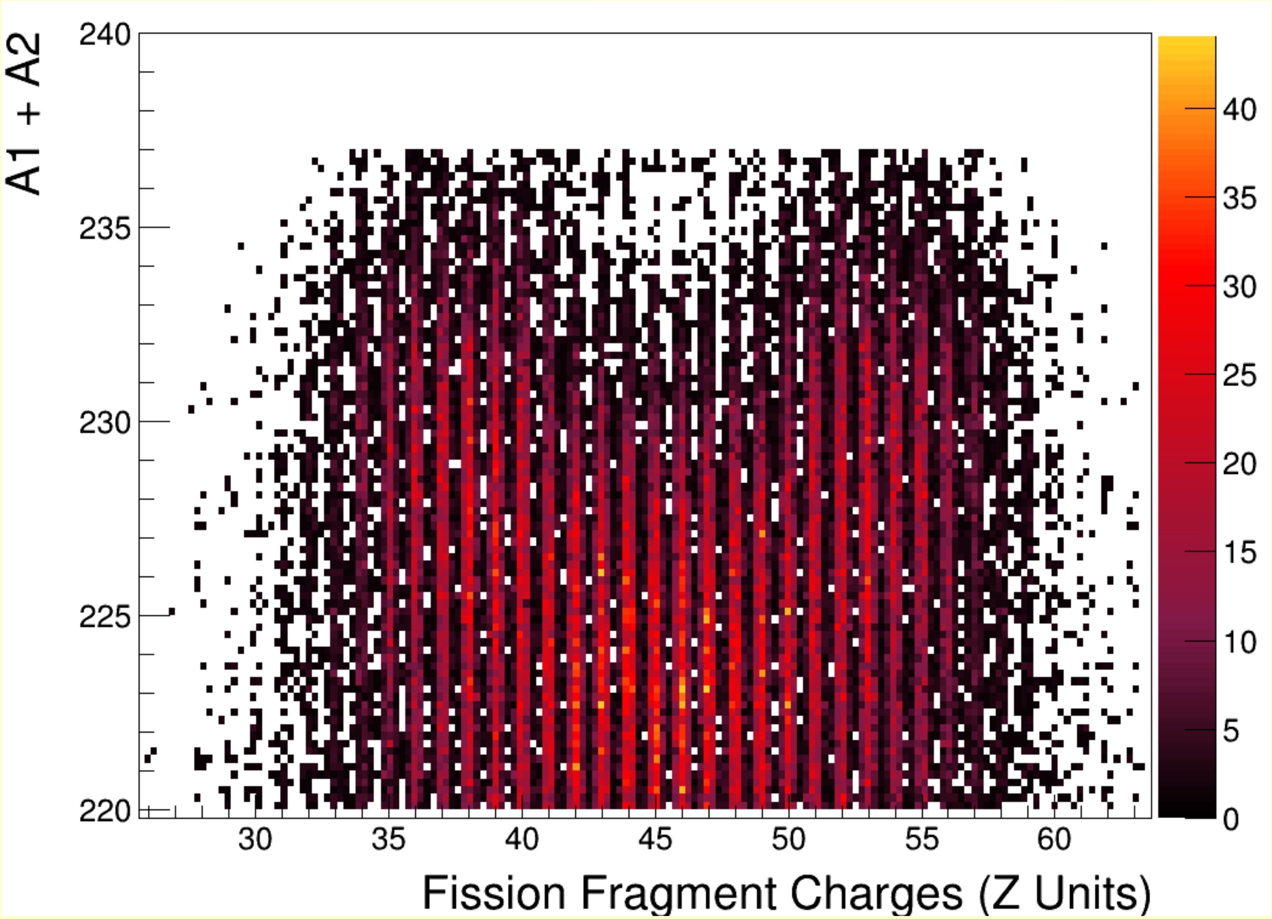

Correlation between the total mass of the fission fragments and its charge distribution !

Higher excitation energy -> More neutron evaporation -> More symmetric fission

A clear transition from asymmetric to symmetric fission when decreasing the total mass (increasing the excitation energy).

Thank you

Full Identification of the Fission Fragments

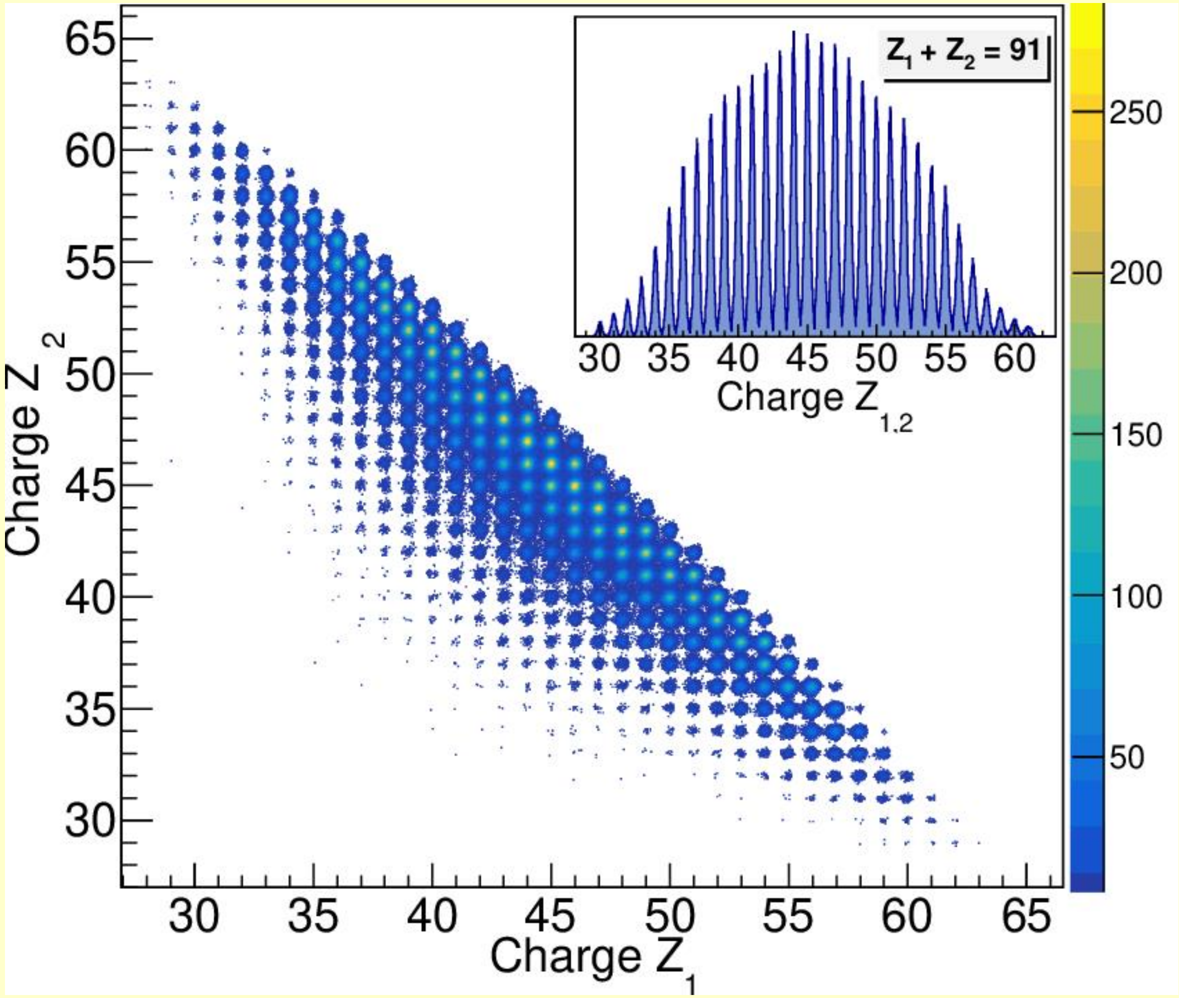

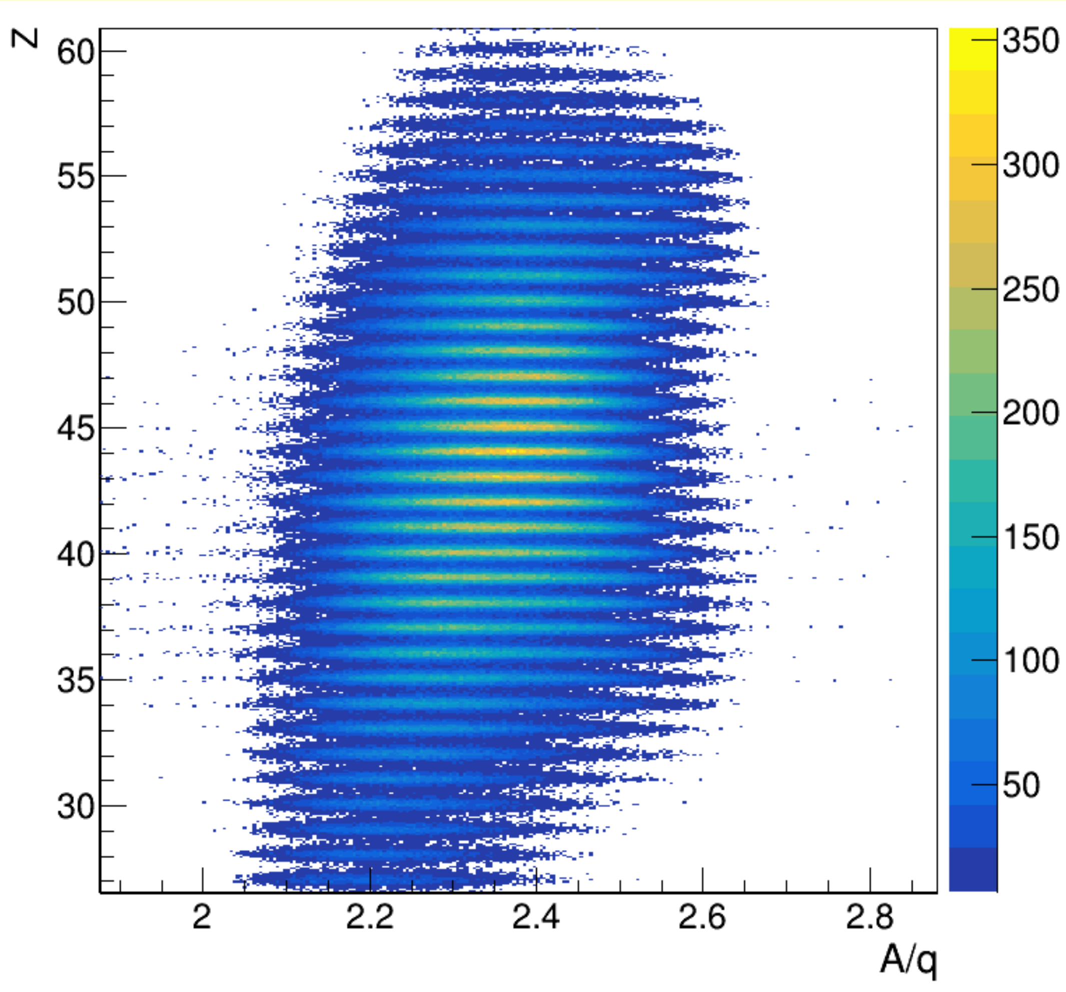

Excellent resolution in atomic number (ΔZ~0.4) but moderate in mass number (ΔA~1.2).

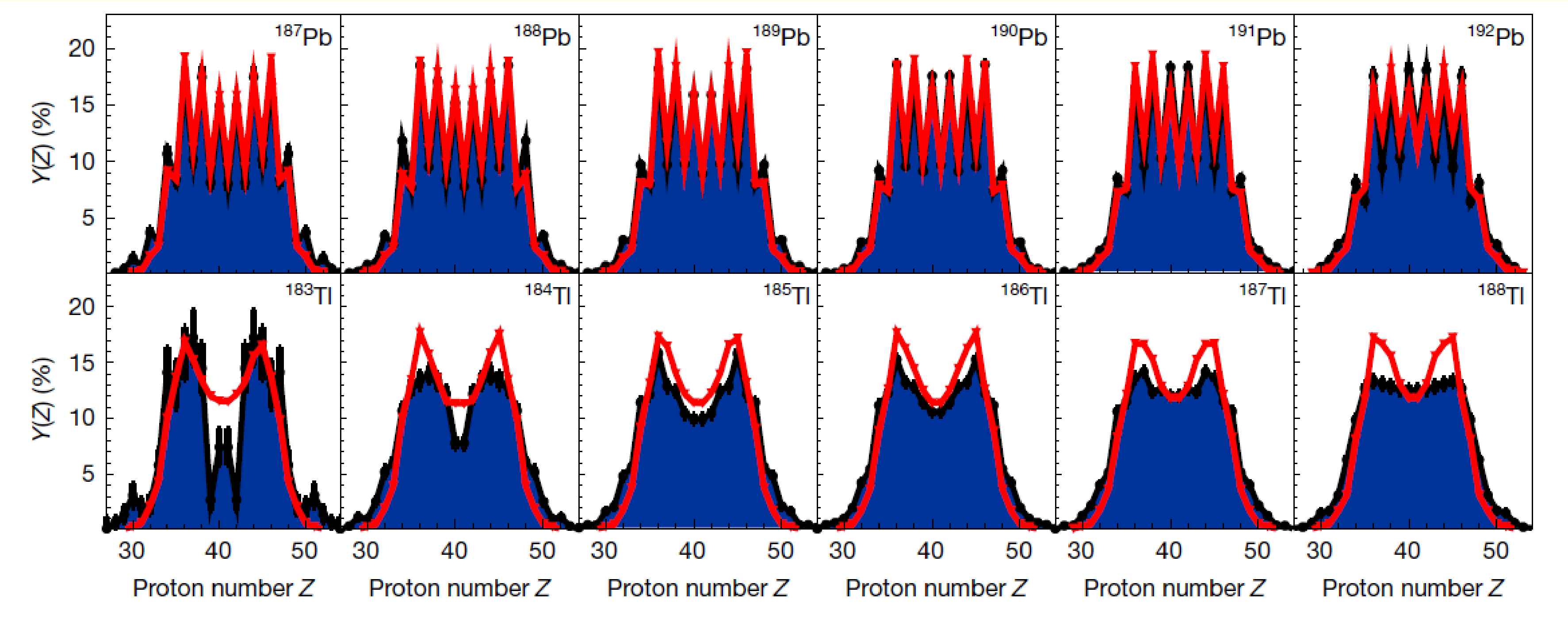

Y(Z) (%)
Proton number Z
^{187}Pb
^{188}Pb
^{189}Pb
^{190}Pb
^{191}Pb
^{192}Pb
^{183}Tl
^{184}Tl
^{185}Tl
^{186}Tl
^{187}Tl
^{188}Tl

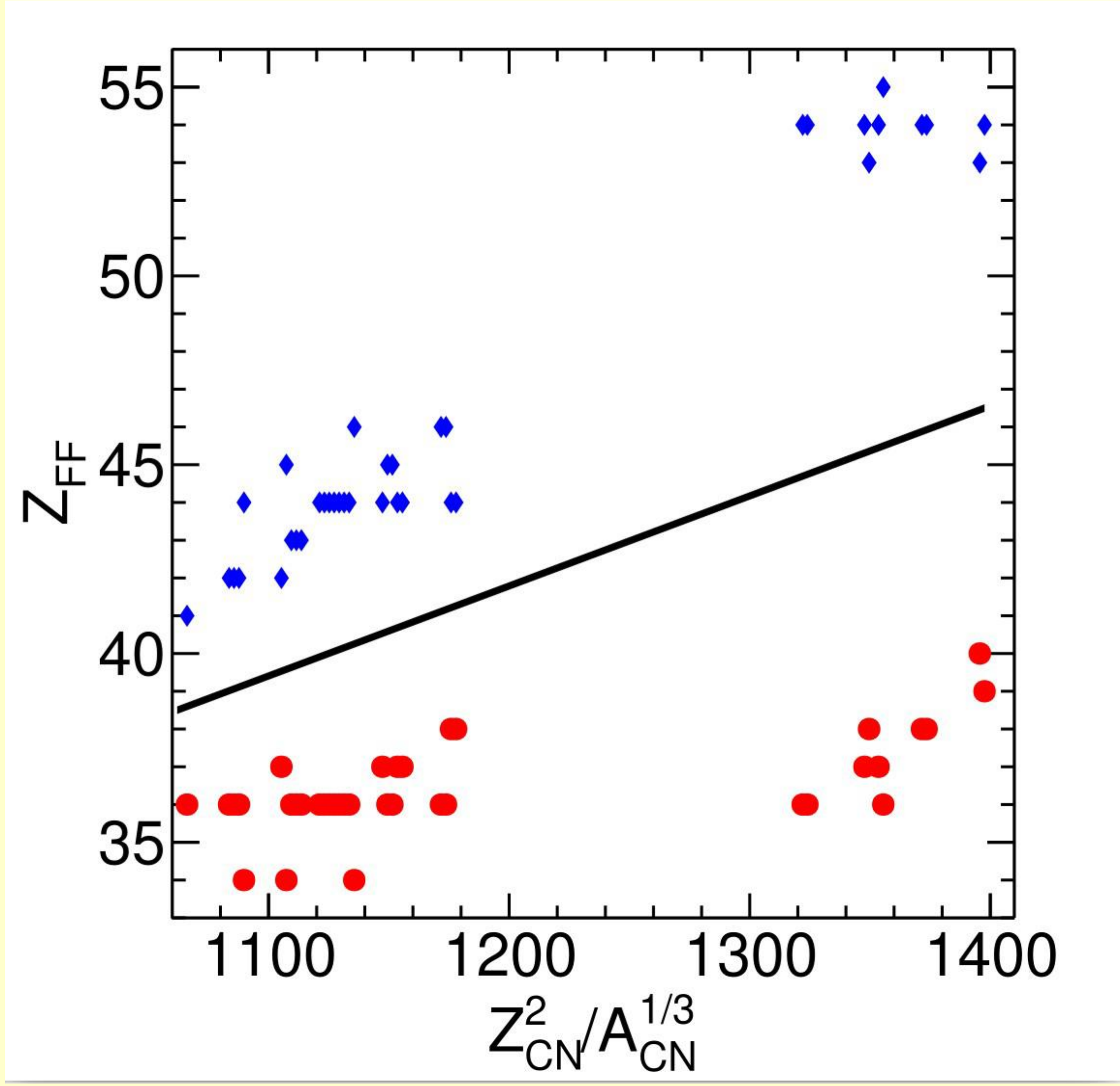

55
50
45
40
35
Z_{FF}
1100
1200
1300
1400
$Z_{CN}^2/A_{CN}^{1/3}$

Discussion on Suppression Factors.

Fission potential

Fission barriers

Damping of shell effects:

- **potential energy**: fission yields
- **level densities collective enhancement**: fission probabilities

Some controversy:

- First proposed by Ignatyuk SJNP-1979

$$S(E^*) = e^{-E^*/\gamma}$$

with γ~15 MeV

- Modified by Randrup PRC-2013

$$S(E^*) = \frac{1 + e^{-E_1/E_0}}{1 + e^{(E^* - E_1)/E_0}}$$

with E_0=15 MeV and E_1=20 MeV

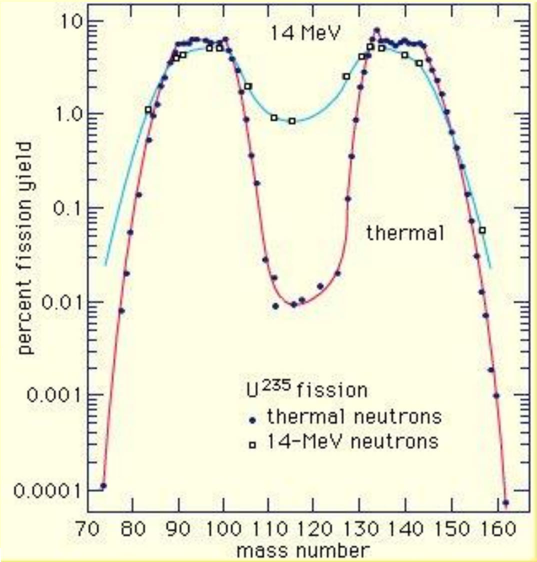

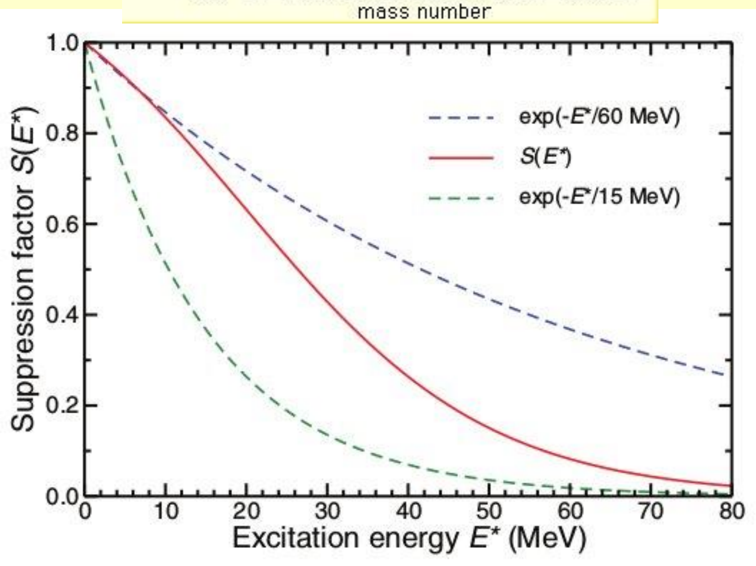

Resolution is Dominated by Tracking

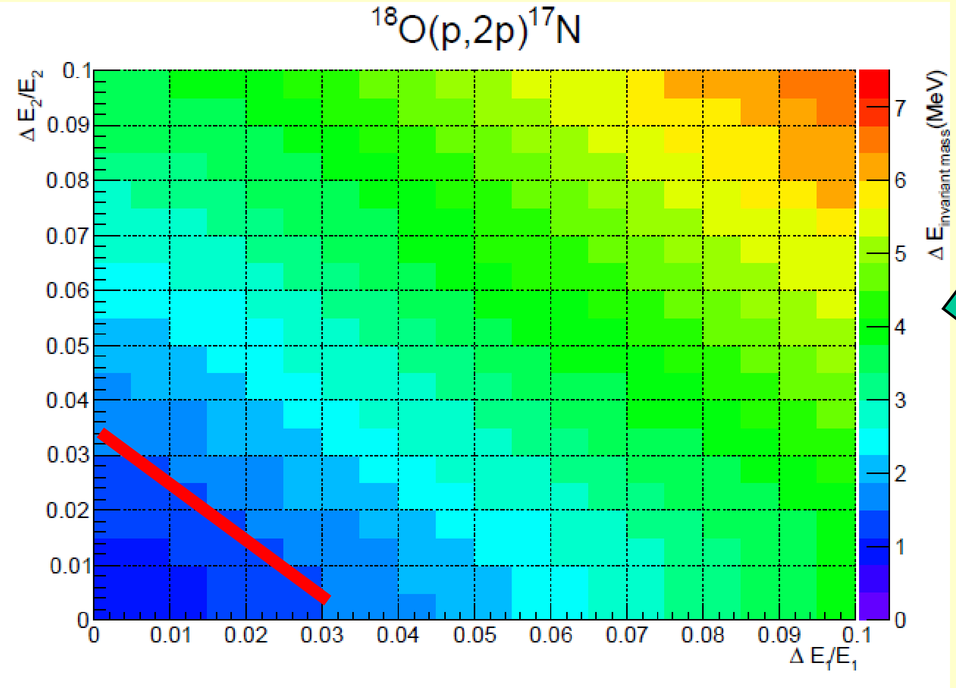

tracking resolution

1 mrad

3 mrad

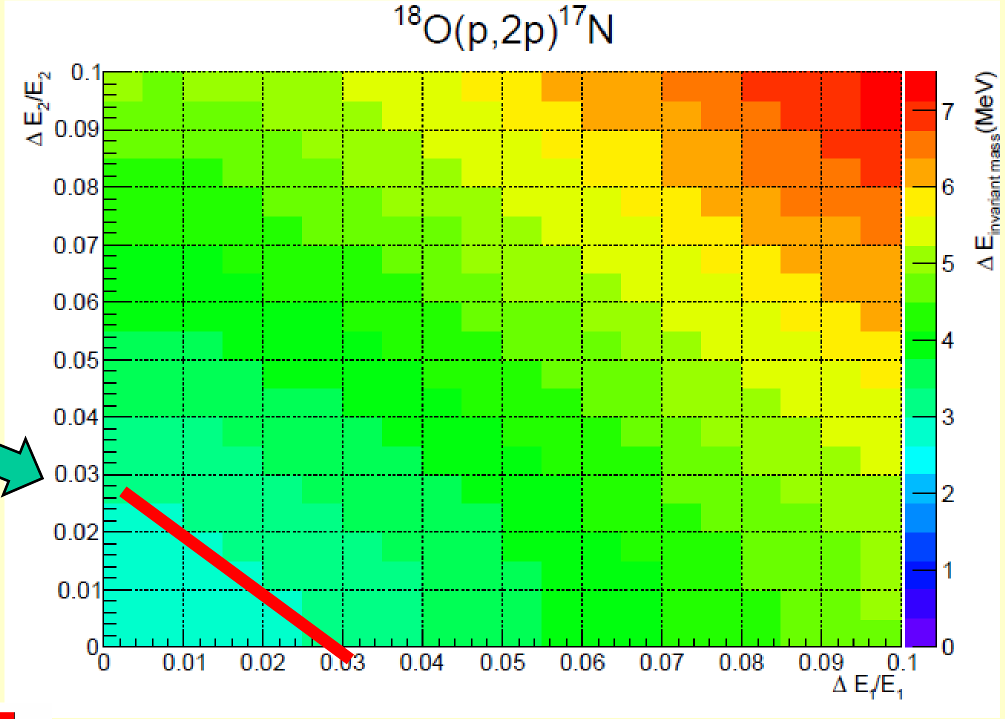

Goal: $\Delta\Theta < 1.2$mrad
$\Delta E/E < 3\ \%$

Simulation:
^{18}O beam at 700 AMeV and thin LH_2 target

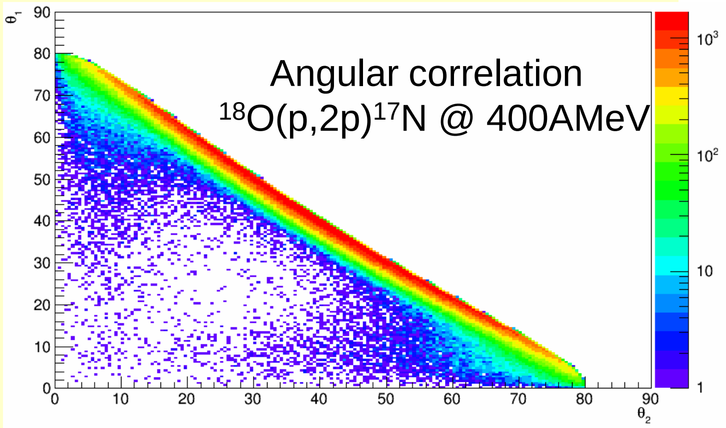

We need:
- minimum material budget
- perfect resolution
- large acceptance
- resilience to delta electrons

The FAIR (in)official Startup Schedule

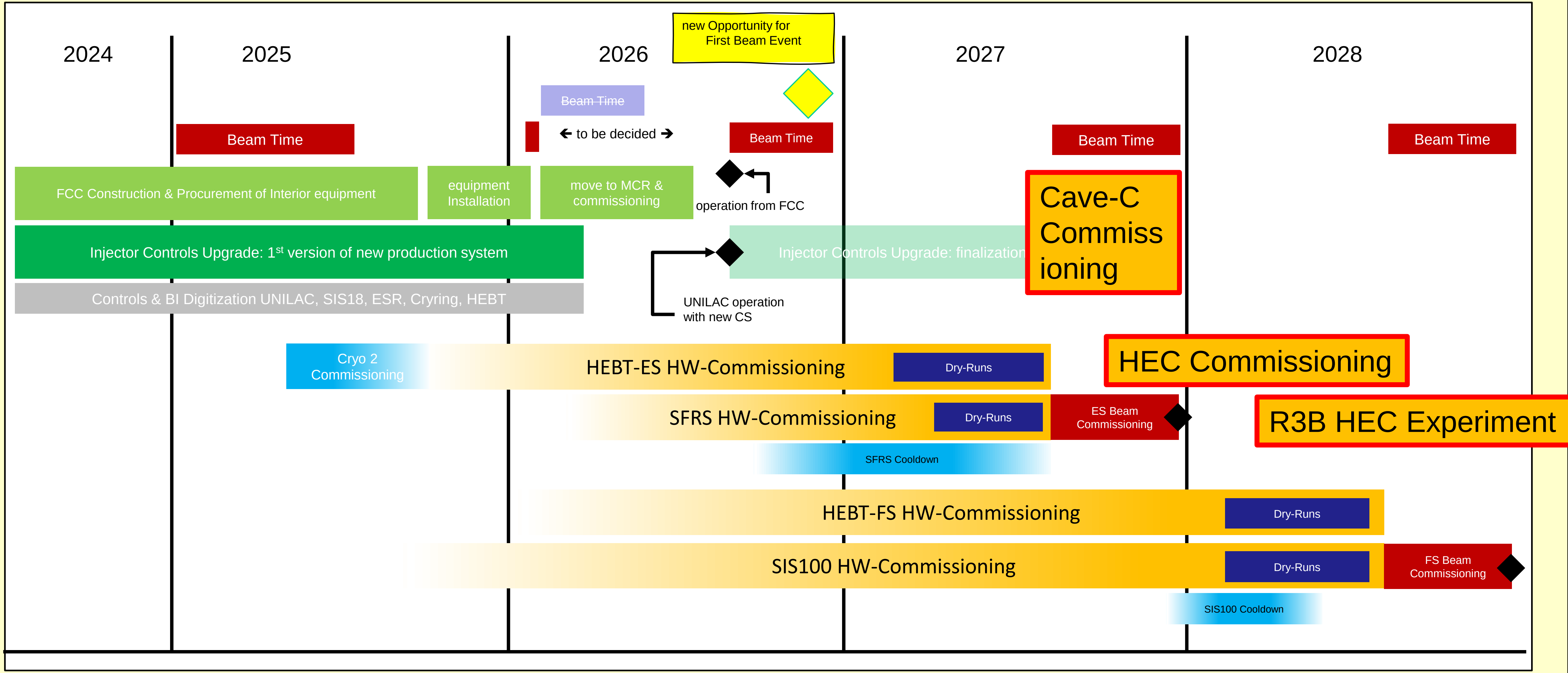

State of the Art for Light Ions

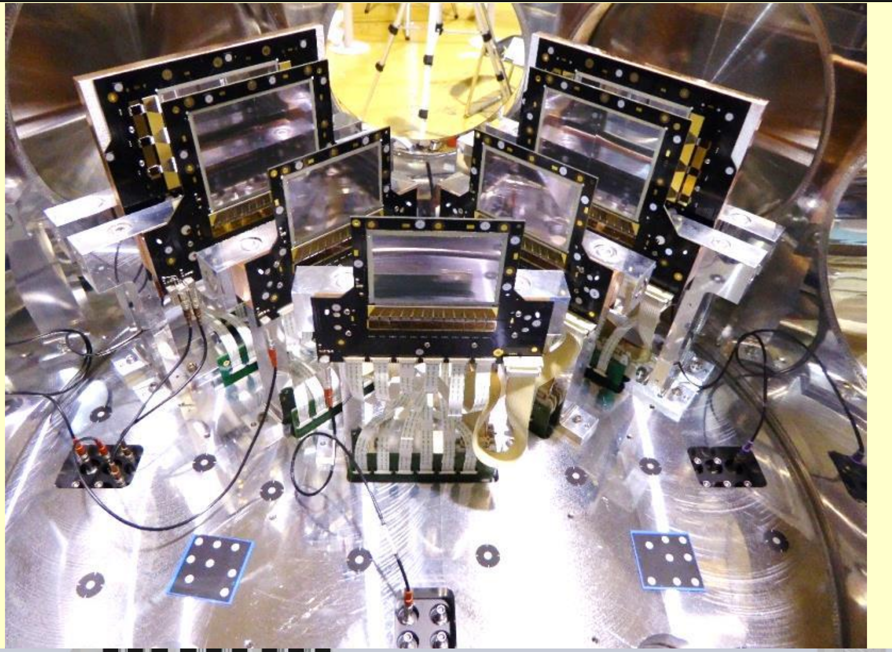

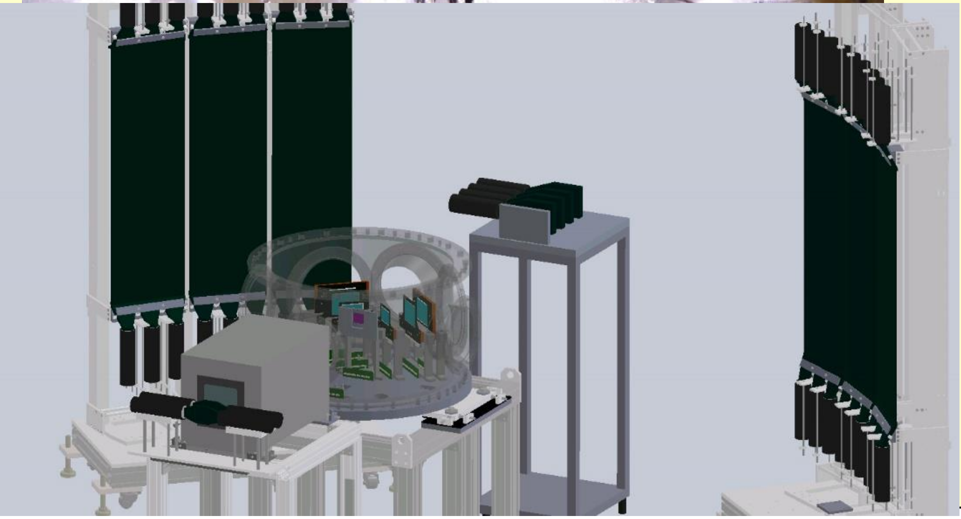

^{16}O at 290 MeV/u with 10^5 pps @ HIMAC

Using 100 μm silicon strip detectors at large distances in a huge vacuum chamber with TOF for the energies at 2 m distance.

Silicon acceptance <1%
Strip detectors produce combinatorial Background (Δe-)

With the exotic beams at FAIR we will have 100 pps beam intensity

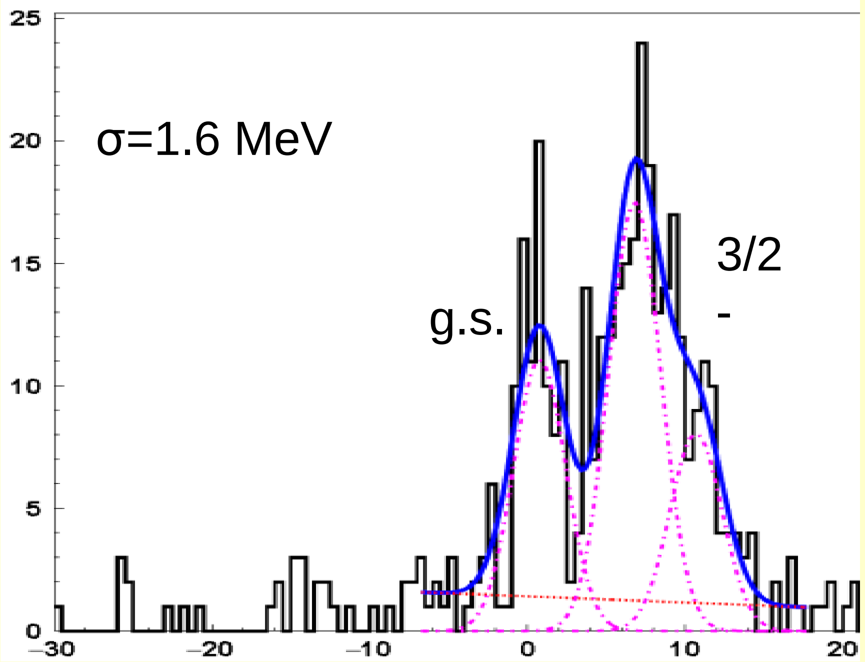

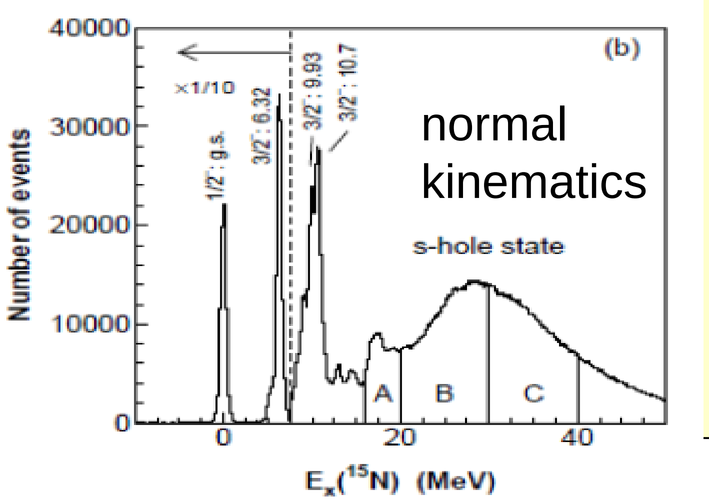

TRT Stage 2 Commissionig 2027 in CAVE-C

Hardware ready spring 2027
Beam time granted for September 2027

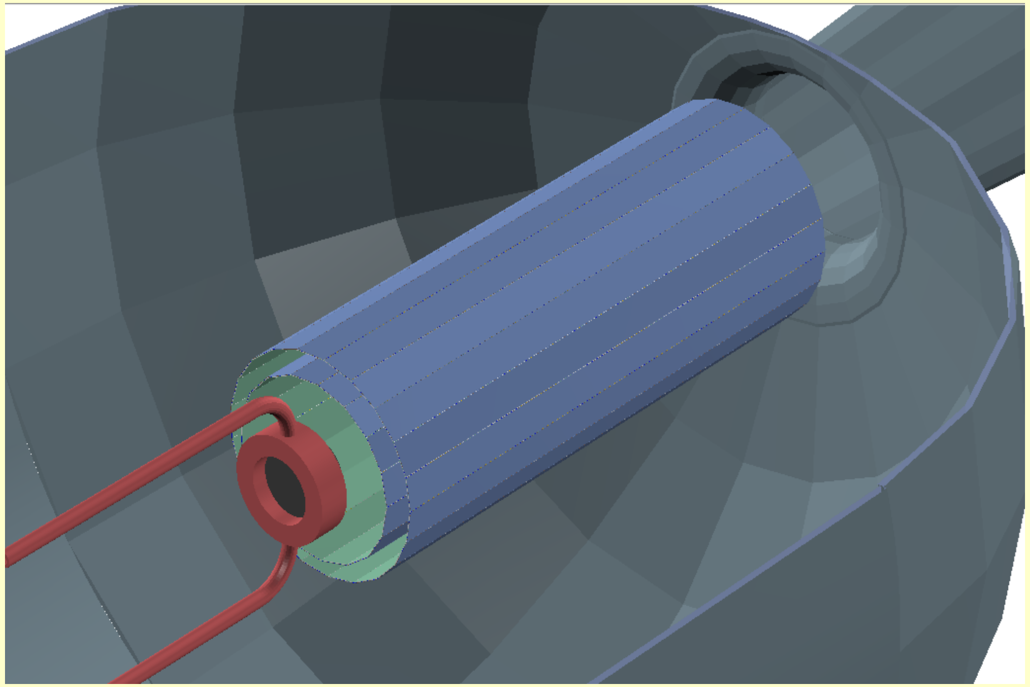

First useful combination of TRT and CALIFA
To determiner the 2p efficiency and missing mass resolution at 2 different energies (400/600 AMeV)

Tasks:
- energy dept. efficiency
- rate dept. efficiency
- cluster algorithm
- combinatorial background
- delta electrons from LH2 with heavy beams
- proton HI separation

Tools:
- H(p,p) elastic scattering $E(\Theta)$ known from the 2nd proton
- In beam detectors at different rates and beam energies.
- $^{238}U(p, 2p)$ or/and Sn(p,2p), for delta electrons

TRT stage1 test for Delta electrons

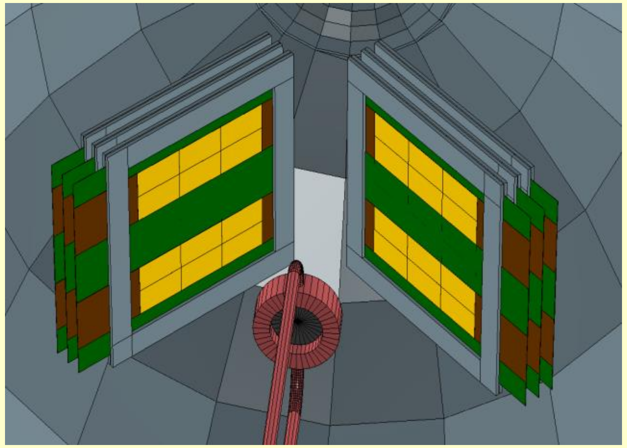

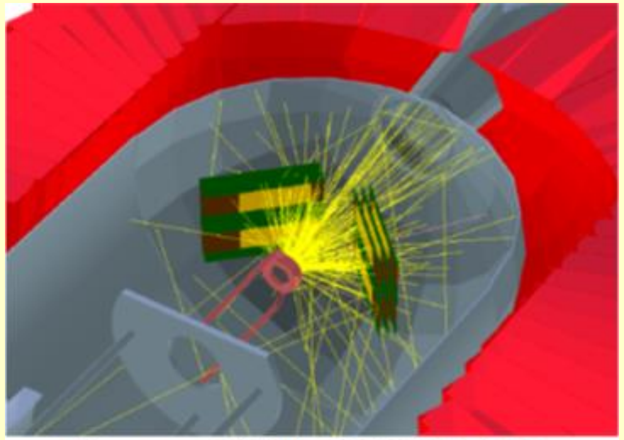

Beam of ^{238}U @ 500MeV/u

Physics Examples

Quenching of proton-removal channels from quasi-free nucleon knockout around ^{132}Sn

QFS reaction with light ions $^{12}C(p,2p)^{11}B^*$, Only final de-excitation, feeding not separated

SRC with stable nuclei.
Is this really N/Z or just size dependendent

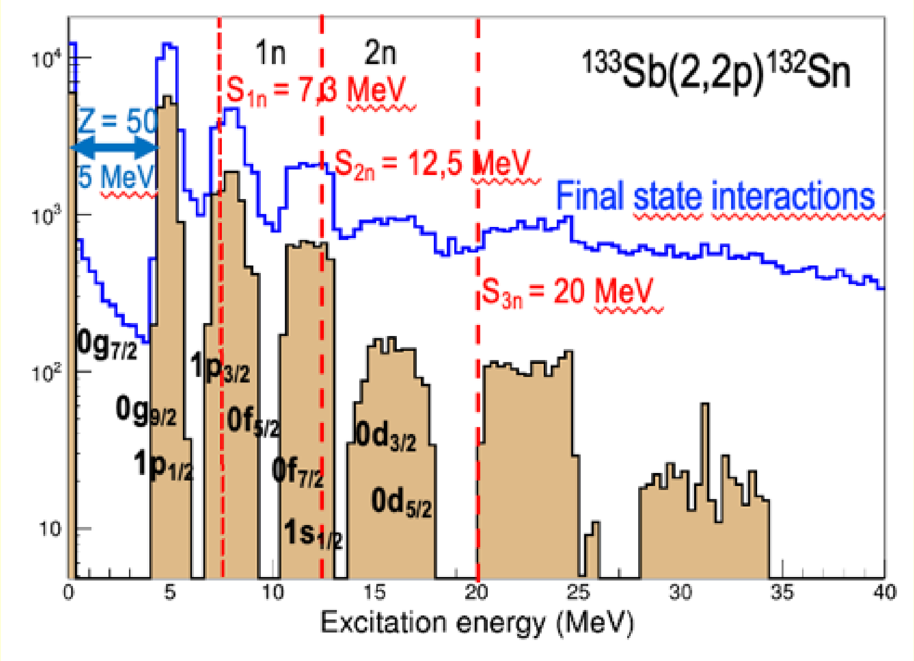

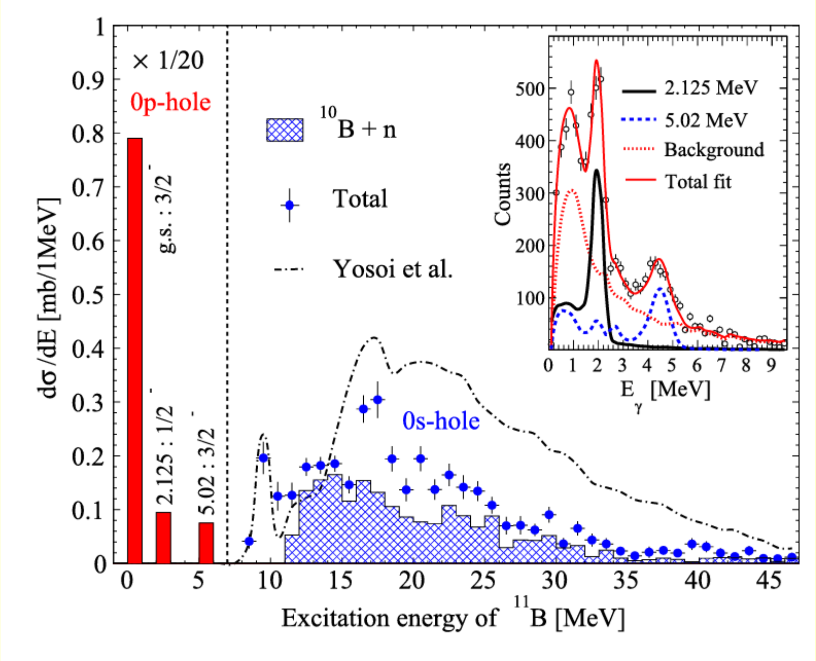

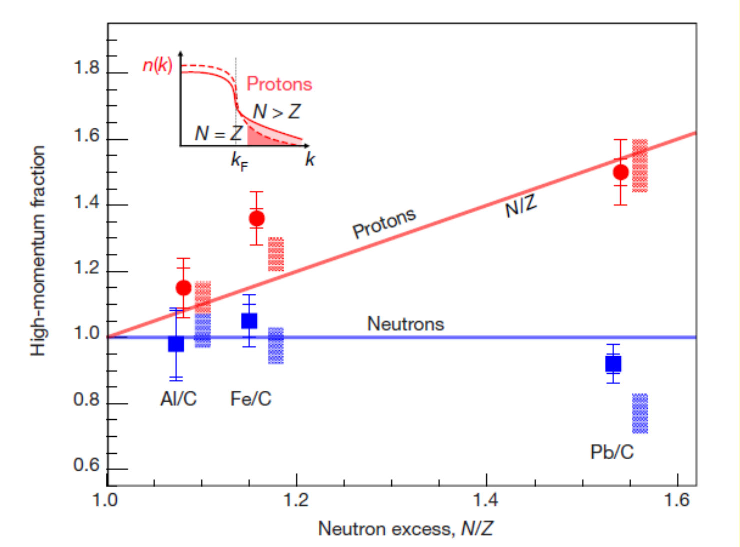

Fig. 11. Experimentally extracted fractions of high- to low-momentum protons (red) and neutrons (blue) for nuclei with different N/Z. The fraction is given relative to ^{12}C. Reprinted from Ref. [75] with permission from Springer.

Simulated proton-hole and final state excitations in $^{133}Sb(p,2p)^{132}Sn$

Panin et al.: Eur. Phys. J. A (2021) 57:103

Panin et al.: Physics Letters B 753 (2016) 204–210